

## Electrical coupling between *Aplysia* bag cell neurons: characterization and role in synchronous firing

Zahra Dargaei,\* Phillip L. W. Colmers,\* Heather M. Hodgson, and Neil S. Magoski

Department of Biomedical and Molecular Sciences, Physiology Graduate Program, Queen's University, Kingston, Ontario, Canada

Submitted 8 July 2014; accepted in final form 29 August 2014

**Dargaei Z, Colmers PL, Hodgson HM, Magoski NS.** Electrical coupling between *Aplysia* bag cell neurons: characterization and role in synchronous firing. *J Neurophysiol* 112: 2680–2696, 2014. First published September 3, 2014; doi:10.1152/jn.00494.2014.—In neuroendocrine cells, hormone release often requires a collective burst of action potentials synchronized by gap junctions. This is the case for the electrically coupled bag cell neurons in the reproductive system of the marine snail, *Aplysia californica*. These neuroendocrine cells are found in two clusters, and fire a synchronous burst, called the afterdischarge, resulting in neuropeptide secretion and the triggering of ovulation. However, the physiology and pharmacology of the bag cell neuron electrical synapse are not completely understood. As such, we made dual whole cell recordings from pairs of electrically coupled cultured bag cell neurons. The junctional current was nonrectifying and not influenced by postsynaptic voltage. Furthermore, junctional conductance was voltage independent and, not surprisingly, strongly correlated with coupling coefficient magnitude. The electrical synapse also acted as a low-pass filter, although under certain conditions, electrotonic potentials evoked by presynaptic action potentials could drive postsynaptic spikes. If coupled neurons were stimulated to spike simultaneously, they presented a high degree of action potential synchrony compared with not-coupled neurons. The electrical synapse failed to pass various intracellular dyes, but was permeable to Cs<sup>+</sup>, and could be inhibited by niflumic acid, meclofenamic acid, or 5-nitro-2-(3-phenylpropylamino)benzoic acid. Finally, extracellular and sharp-electrode recording from the intact bag cell neuron cluster showed that these pharmacological uncouplers disrupted both electrical coupling and afterdischarge generation in situ. Thus electrical synapses promote bag cell neuron firing synchrony and may allow for electrotonic spread of the burst through the network, ultimately contributing to propagation of the species.

gap junction; junctional current; afterdischarge; neuroendocrine cell; mollusk

ELECTRICAL SYNAPSES, OR GAP junctions, are intercellular channels that permit ionic current and other solutes to flow between neurons (Bennett 1966, 1977, 2000). Originally considered as a means to link invertebrate neurons for dependable and rapid signaling during escape responses (Furshpan and Potter 1959), it is now established that electrical synapses facilitate and/or synchronize neuronal activity in circuits controlling sensory, motor, and neuroendocrine function in both vertebrate (Gibson et al. 1999; Landisman et al. 2002; Solomon et al. 2003; Bennett and Zulkun 2004; McCracken and Roberts 2006; Desarménien et al. 2013) and invertebrate (Getting and Willows

1974; Carew and Kandel 1977; De Vlieger et al. 1980; Spencer 1981; Benjamin and Pilkington 1986; Norekian 1999; Ermentrout et al. 2004; Cao and Nitabach 2008; Sieling et al. 2014; Wu et al. 2014) nervous systems.

Reproduction in the anaspidean marine mollusk, *Aplysia californica*, is governed by the bag cell neurons, a group of neuroendocrine cells found in two clusters anterior to the abdominal ganglion (Kupfermann et al. 1966; Kupfermann and Kandel 1970; Conn and Kaczmarek 1989). In response to cholinergic and peptidergic input, the bag cell neurons fire a lengthy burst of action potentials, called an afterdischarge, to release egg-laying hormone at an adjacent neurohemal area (Coggeshall 1967; Frazier et al. 1967; Arch 1972; Brown et al. 1989; White and Magoski 2012; White et al. 2014). This peptide hormone acts on other neurons in the brain as well as the ovotestis to trigger egg-laying behavior (Mayeri et al. 1979a,b; Stuart and Strumwasser 1980; Rothman et al. 1983). Prior work shows that the afterdischarge represents the synchronous firing of all bag cell neurons in both clusters (Kupfermann and Kandel 1970; Blankenship and Haskins 1979; Kaczmarek et al. 1979; Haskins and Blankenship 1979). These findings, from *A. californica* as well as *A. brasiliana* and *A. dactylorella*, suggest synchrony is due to electrical coupling within and between the clusters, although the properties of these junctions are poorly defined.

The electrical synapses connecting bag cell neurons in the intact cluster appear to be electrotonically distant, and the neurons are probably linked to multiple partners (Kupfermann and Kandel 1970; Blankenship and Haskins 1979). To an extent, this has restricted further examination of coupling in the intact ganglion; consequently, we sought to characterize the electrical synapse between pairs of cultured bag cell neurons and then apply those findings to assess the role of these connections in the afterdischarge. Two previous reports have looked at electrical coupling in cultured bag cell neurons; however, those inquiries were largely confined to recordings of coupling coefficient (Kaczmarek et al. 1979; Lin and Levitan 1987). In the present study, we use current and voltage clamp to demonstrate that the bag cell neuron electrical synapse is voltage independent, behaves as a low-pass filter, shows limited permeability, and is sensitive to certain gap junction blockers; moreover, coupling seems essential for both action potential synchrony and the afterdischarge itself. This is consistent with other neuroendocrine systems, where gap junctions coordinate collective firing and hormone secretion to regulate circulating catecholamine levels, circadian rhythms, lactation, parturition, or ovulation (Andrew et al. 1981; Summerlee 1981;

\* Z. Dargaei and P. L. W. Colmers contributed equally to this work.

Address for reprint requests and other correspondence: N. S. Magoski, Dept. of Biomedical and Molecular Sciences, Queen's Univ., 4th Floor, Botterell Hall, 18 Stuart St., Kingston, ON, K7L 3N6, Canada (e-mail: magoski@queensu.ca).

Belin and Moos 1986; Colwell 2000; Martin et al. 2001; Vazquez-Martinez et al. 2001; Long et al. 2005).

## MATERIALS AND METHODS

**Animals and cell culture.** Adult *Aplysia californica* (a hermaphrodite) weighing 150–500 g were obtained from Marinus (Long Beach, CA) and housed in an ~300-liter aquarium containing continuously circulating, aerated sea water (Instant Ocean; Aquarium Systems, Mentor, OH) at 14–16°C on a 12:12-h light-dark cycle and fed romaine lettuce five times per week. All experiments were approved by the Queen's University Animal Care Committee (Protocols Magoski-100323 or Magoski-100845).

For primary cultures of isolated bag cell neurons, animals were anesthetized by an injection of isotonic MgCl<sub>2</sub> (50% of body wt), the abdominal ganglion was removed and treated with Dispase II (13.3 mg/ml; 165859; Roche Diagnostics, Indianapolis, IN) dissolved in tissue culture artificial sea water (tcASW) (composition in mM: 460 NaCl, 10.4 KCl, 11 CaCl<sub>2</sub>, 55 MgCl<sub>2</sub>, 15 HEPES, 1 mg/ml glucose, 100 U/ml penicillin, and 0.1 mg/ml streptomycin, pH 7.8 with NaOH) for 18 h at 22°C. The ganglion was then rinsed in tcASW for 1 h, and the bag cell neuron clusters were dissected from their surrounding connective tissue. With the use of a fire-polished glass Pasteur pipette and gentle trituration, neurons were dissociated and dispersed in tcASW onto 35 × 10 mm polystyrene tissue culture dishes (353001; Falcon Becton-Dickinson, Franklin Lakes, NJ). In a few instances, cells were plated onto glass coverslips (#1; 12–542-B; Fisher Scientific, Ottawa, ON, Canada) coated with 20 μg/ml poly-L-lysine hydrobromide, molecular weight = 300,000 (P1524; Sigma-Aldrich, Oakville, ON, Canada) that were glued with Sylgard (SYLG184; World Precision Instruments, Sarasota, FL) over holes drilled out of the bottom of the tissue culture dish. Neurons were paired manually by bringing a free neuron into contact with a neuron already adhered to the dish. This was achieved by triturating fluid to either push or pull the free neuron and place it next to the adhered neuron. Neurons were typically plated either with their somata (soma-soma) or primary neurites (neurite-neurite) in contact; in some cases, to act as a control, neurons were separated by a maximum distance of one soma diameter, without neurites touching. Cultures were maintained in a 14°C incubator in tcASW and used for experimentation within 1–3 days. Salts were obtained from Fisher, ICN (Aurora, OH) or Sigma-Aldrich.

**Whole cell voltage- and current-clamp recordings from cultured bag cell neurons.** Recordings of membrane potential or current were made from cultured bag cell neurons using EPC-8 amplifiers (HEKA Electronics; Mahone Bay, NS, Canada) and the tight-seal, whole cell method (Hamill et al. 1981). Microelectrodes were pulled from 1.5-mm external diameter/1.2-mm internal diameter, borosilicate glass capillaries (TW150F-4; World Precision Instruments) and had a resistance of 1–3 MΩ when filled with regular intracellular saline [composition in mM: 500 K<sup>+</sup>-aspartate, 70 KCl, 1.25 MgCl<sub>2</sub>, 10 HEPES, 11 glucose, 10 glutathione, 5 ethylene glycol bis(aminoethyl ether) tetraacetic acid (EGTA), 5 ATP (grade 2, disodium salt; A3377; Sigma-Aldrich), and 0.1 GTP (type 3, disodium salt; G8877; Sigma-Aldrich); pH 7.3 with KOH]. The free Ca<sup>2+</sup> concentration was set at 300 nM by adding 3.75 mM CaCl<sub>2</sub>, as calculated by WebMaxC (<http://www.stanford.edu/~cpatton/webmaxcS.htm>).

In pairs of cultured bag cell neurons, cells were designated as *neuron 1* and *neuron 2*, based on being recorded with the left and right amplifier, respectively. Protocols were run with *neuron 1* as presynaptic and *neuron 2* as postsynaptic and then typically vice versa. Most recordings were done in normal ASW (nASW) (composition as per tcASW, but with glucose and antibiotics omitted) at room temperature (20–22°C). Some experiments employed Ca<sup>2+</sup>-free/high-Mg<sup>2+</sup> ASW (as per nASW but CaCl<sub>2</sub> replaced equimolar with MgCl<sub>2</sub>). The regular intracellular saline had a calculated liquid junction potential of 15 mV vs. both nASW and Ca<sup>2+</sup>-free/high-Mg<sup>2+</sup> ASW, which was corrected by offline subtraction. In a small number of experiments, voltage-

gated K<sup>+</sup> currents were recorded in *neuron 2*; specifically, while voltage clamping *neuron 1* at –40 mV, K<sup>+</sup> currents were elicited in *neuron 2* by stepping from –40 mV to +30 mV for 200 ms. In this case, a Na<sup>+</sup>-free/Ca<sup>2+</sup>-free ASW (composition in mM: 471 NMDG, 10.4 KCl, 66 MgCl<sub>2</sub>, and 15 HEPES; pH 7.8 with KOH) was used as the extracellular saline. Pipettes were filled with either regular intracellular saline (junction potential of 23 mV vs. Na<sup>+</sup>-free/Ca<sup>2+</sup>-free ASW) or saline where the K<sup>+</sup>-aspartate was replaced equimolar with either Cs<sup>+</sup>-aspartate (BP210100; Fisher; junction potential of 23 mV) or tetraethylammonium-Cl (TEA; AC15090; Acros Organics, Morris Plains, NJ; junction potential of 3 mV). Offline subtraction was again used to correct for junction potentials, where as leak current was corrected online using a P/4 protocol from –40 mV, with subpulses of opposite polarity and one-fourth the magnitude of the test pulse to +30 mV, an intersubpulse interval of 500 and 100 ms before the actual test pulse. The leak current evoked by the subpulses was summed, inverted, and subtracted from the current elicited during the test step to derive the voltage-dependent current (Bezanilla and Armstrong 1977).

For all whole cell recordings, pipette junction potentials were nulled immediately before seal formation. Following membrane rupture, pipette and neuronal capacitive currents were cancelled, and the series resistance (3–5 MΩ) was compensated to 70–80% and monitored throughout the experiment. Input signals were low-pass filtered at 1 kHz (for current) and 5 kHz (for voltage) by the EPC-8 Bessel filter and sampled at 2 kHz using an IBM-compatible personal computer, a Digidata 1322A analog-to-digital converter (Molecular Devices; Sunnyvale, CA), and the Clampex acquisition program of pCLAMP 8.1 (Molecular Devices). Clampex was also used to control the membrane potential under voltage clamp and inject current in current clamp; in addition, neurons were manually set to –60 mV in current clamp by delivering constant bias current with the EPC-8 V-hold.

**Intracellular dye staining and fluorescence microscopy of cultured bag cell neurons.** The possibility of dye coupling between electrically coupled bag cell neurons was investigated by staining one cell of a given pair with sulforhodamine 101 (S-359; Invitrogen, Burlington, ON, Canada), carboxyfluorescein (C194; Invitrogen), or biocytin (B-1592; Invitrogen). For sulforhodamine or carboxyfluorescein, the individual dyes were dissolved in regular intracellular saline at 0.1 or 0.5% (wt/vol) and loaded under whole cell voltage clamp at –60 mV. In most cases, the second neuron was also voltage clamped at –60 mV but using a pipette containing intracellular saline with no added dye. Neurons were dye loaded for 30 min, by which time the soma of the cell was the same color as the electrode under appropriate fluorescent light (see below). Photomicroscopy (see below) of neurons stained with sulforhodamine or carboxyfluorescein was usually carried out at the end of the recording period, with the electrode(s) still in place. However, in a few instances, electrodes were successfully withdrawn, the dish was placed in the 14°C incubator overnight, and documentation was performed the next day.

For biocytin, the tips of sharp microelectrodes pulled from 1.2-mm external diameter/0.9-mm internal diameter borosilicate glass capillaries (TW120F-4; World Precision Instruments) were filled with dye in water at 4% (wt/vol). When backfilled with 0.5 M KCl, these electrodes had a resistance of 2–7 MΩ. One neuron from a given pair, plated on glass coverslip dishes, was impaled and the membrane potential (typically –50 mV to –60 mV) was monitored with an Axoclamp 2B amplifier (Molecular Devices). Microelectrodes were bridge balanced with a Grass S88 stimulator (Astro-Med, Longueuil, QC, Canada) and dye injected for 20 min. Injection was by ionophoresis similar to Ewadding et al. (1994) and Fan et al. (2005); specifically, the Axoclamp DC current command was used to depolarize the neuron to approximately –30 mV, while the stimulator simultaneously injected 500-ms negative current steps at 0.1–0.5 Hz to periodically hyperpolarize the cell to approximately –90 mV. The electrode was then withdrawn and the dish placed in the 14°C

incubator overnight; the next day, neurons were fixed for 25 min in 4% (wt/vol) paraformaldehyde (04042; Fisher) in 400 mM sucrose/nASW (pH 7.5 with NaOH), permeabilized for 5 min with 0.3% (wt/vol) Triton X-100 (BP151; Fisher) in fix, and washed four times with PBS (composition in mM: 137 NaCl, 2.7 KCl, 4.3 Na<sub>2</sub>HPO<sub>4</sub>, and 1.5 KH<sub>2</sub>PO<sub>4</sub> pH 7.0 with NaOH). Neurons were then incubated overnight in the dark at 4°C in streptavidin-Alexa Fluor 488 conjugate (S-32354; Invitrogen) (1:100 in PBS), washed the next day four times with PBS, mounted in mounting solution [26% wt/vol glycerol (BP2291; Fisher), 11% wt/vol Mowiol 4–88 (17951; Polysciences, Warrington, PA), and 110 mM TRIS (pH 8.5)], and covered with a glass coverslip.

Stained neurons were imaged with a Nikon TS100-F inverted microscope (Nikon, Mississauga, ON, Canada), equipped with a Nikon Plan Fluor 20× (numerical aperture 0.50) objective and a 50-W Hg lamp. For carboxyfluorescein or Alexa Fluor 488, excitation was provided by a 480/15-nm band pass filter, and the fluorescence was emitted to the eyepiece or camera through a 505-nm dichroic mirror and 520-nm barrier filter. Sulforhodamine was excited with a 535/25-nm band-pass filter, and the emitted light passed through a 575-nm dichroic mirror and 590-nm barrier filter. Images (1,392 × 1,040 pixels) were acquired at the mid-level focal plane on the vertical axis of the soma using a Pixelfly USB camera (Photon Technology International, London, ON, Canada) and the Micro-Manager 1.4.5 plugin (<http://micro-manager.org>) for ImageJ 1.44n9 (<http://rsbweb.nih.gov/ij/>) with 100- to 500-ms exposure times.

*Ensemble, extracellular, and sharp-electrode, current-clamp recording from the intact bag cell neuron cluster.* To record afterdischarges from the intact bag cell neuron cluster, the abdominal ganglion was removed as per *Animals and cell culture*. Ganglia were pinned ventral surface up in nASW to the bottom of a Sylgard-lined 35 × 10 mm tissue culture, which served as the bath, and maintained at 14°C using an Isotemp circulating chiller (3016; Fisher). A wide-bore, fire-polished glass suction recording electrode (containing nASW) was placed over the right bag cell neuron cluster, while a similar stimulating electrode was placed at the rostral end of the right pleuroabdominal connective. Stimulating current pulses were delivered with a Grass SD9 stimulator while voltage was monitored using a DP-301 differential amplifier (Warner Instruments; Hamden, CT). Voltage was high-pass filtered at 0.1 Hz and low-pass filtered at 1 kHz using the DP-301 filters and acquired at a sampling rate of 2 kHz using the Digidata 1322A and Axoscope 9.0 (Molecular Devices).

For intracellular recording from bag cell neurons in the intact cluster, the sharp-electrode, bridge-balance method was again employed but in this case using two Neuroprobe 1600 amplifiers (A-M Systems, Sequim, WA). To facilitate sharp-electrode impalement, ganglia were treated with 0.5 mg/ml elastase (E1250; Sigma-Aldrich) and 1 mg/ml collagenase/dispase (10269638001; Roche Diagnostics) for 2 h, followed by three 10-min washes in nASW alone. The left bag cell neuron cluster was then desheathed using fine forceps. Electrodes (as per *Intracellular dye staining and fluorescence microscopy of cultured bag cell neurons*) had resistances of 10–20 MΩ when filled with 2 M K<sup>+</sup>-acetate plus 10 mM HEPES and 100 mM KCl (pH 7.3 with KOH). Microelectrodes were bridge balanced with a Grass S88 stimulator and stimulus current injected into the neurons via the Neuroprobe 1600 momentary current injection function. Voltage was filtered at 5 kHz using the Neuroprobe low-pass filter and acquired with the Digidata and Axoscope at 2 kHz.

*Drug application and reagents.* Almost all solution exchanges were accomplished using a calibrated transfer pipette to first replace the bath (culture dish) tcASW with the desired extracellular saline. Drugs were introduced by initially removing a small volume (~75 μl) of saline from the bath, combining that with an even smaller volume (<10 μl) of drug stock solution and then reintroducing that mixture back into the bath. Care was taken to pipette near the side of the dish and as far away as possible from the neurons. In one set of experiments, rapid perfusion was used to wash in and then wash out certain

drugs. This involved an ~500-μm bore micromanipulator-controlled square-barrelled glass pipette, connected by tubing and a stopcock manifold to a series of gravity-driven reservoirs. The pipette was positioned 500–700 μm from the somata of neuronal pairs and delivered a constant flow over the neurons of ~1 ml/min. Niflumic acid (N0630; Sigma-Aldrich), meclofenamic acid (M4531; Sigma-Aldrich), 5-nitro-2-(3-phenylpropylamino)benzoic acid (N4779; Sigma-Aldrich), and 18-α-glycyrrhetic acid (G8503; Sigma-Aldrich) were dissolved as stocks in dimethyl sulfoxide (DMSO; BP231–1; Fisher). Quinine (Q1250; Sigma-Aldrich) stock was dissolved in ethanol. The maximal final concentration of DMSO or ethanol ranged from 0.05 to 0.5% (vol/vol), which in control experiments had no effect on holding current, membrane conductance, or junctional current. Prior work from our laboratory has found that these vehicles do not alter bag cell neuron macroscopic or single-channel currents, membrane potential, membrane capacitance, or intracellular Ca<sup>2+</sup> (Magoski et al. 2000; Magoski and Kaczmarek 2005; Kachoei et al. 2006; Lupinsky and Magoski 2006; Hung and Magoski 2007; Gardam et al. 2008; Geiger and Magoski 2008; Tam et al. 2009, 2011; Hickey et al. 2010, 2013). We also attempted to employ carbenoxolone (C4790; Sigma-Aldrich) but were unable to dissolve it into nASW from either a DMSO- or ethanol-based stock.

*Data analysis.* The majority of analysis involved pairs of bag cell neurons (*neuron 1* and *neuron 2*) with respective membrane potentials and membrane currents specified as *V1*, *V2*, *I1*, and *I2*. The Clampfit (8.1 or 10.2) analysis program of pCLAMP was used to determine the amplitude and time course of membrane current or voltage. For current, a cursor was placed at an average point along the baseline, before any voltage step, and at the steady-state current response during the step. Current was taken within 20 ms of the end of the test step. Similarly, for voltage, a cursor was again placed at the baseline, before a current step, and at the steady-state membrane potential seen during a hyperpolarizing pulse or postsynaptic response. In both cases, the difference between the two cursor values was taken as the amplitude of the response.

Membrane conductance was determined by taking the difference between a given test voltage step delivered to *neuron 1* and the –60-mV holding potential (*V1* – –60 mV) and then dividing that into the steady-state current (*I1*) evoked by the test voltage (*I1*/(*V1* – –60 mV)) and vice versa (*I2*/(*V2* – –60 mV)). Junctional conductance was calculated by dividing the steady-state current in *neuron 2* (*I2*) by the junctional voltage, i.e., the difference between the postsynaptic holding potential and the presynaptic test voltage step (*I2*/(–60 mV – *V1*)) and vice versa (*I1*/(–60 mV – *V2*)). Both membrane conductance and junctional conductance were plotted against the test voltage using Prism 6.0 (GraphPad Software; La Jolla, CA), which was also used to fit membrane conductance voltage relationships with a Boltzmann sigmoid. The filter function of the electrical synapse was examined by determining the attenuation over time of the peak voltage response seen in a current clamped neuron to a test pulse applied at 1, 5, or 10 Hz to a coupled partner under voltage clamp. Attenuation at all frequencies was also normalized to that at 1 Hz. Coupling coefficient was ascertained by the ratio of *V2*/*V1* or *V1*/*V2* at the steady-state membrane potential after a hyperpolarizing current pulse to *neuron 1* or *neuron 2*, respectively. Times of peak voltage change were determined automatically by placing cursors before and after an action potential in one neuron as well as the corresponding electrotonic potential (ETP) in the second neuron. The peak-to-peak latency between action potential and ETP was calculated as the difference between these times. Firing synchrony was measured by comparing the time-shifted data between pairs of firing neurons using the cross-correlation analysis function in Clampfit with the number of lags at ± 1,000. Finally, the effectiveness of gap junction blockers was expressed by calculating the percent change in junctional current following addition of vehicle or drug.

Statistics were performed using Prism or InStat 3.1 (GraphPad Software). Data are presented as the means ± SE. Prism was also used

for linear regression analysis. The Kolmogorov-Smirnov method was used to test data sets for normality. For normally distributed data, Student's unpaired *t*-test was used to test for differences between two means, while an ordinary one-way ANOVA with either the Dunnett or Tukey-Kramer multiple comparisons test was used to test for differences between multiple means. For some data sets, the one-way ANOVA was followed instead by a test for linear trend, which determines if the column means change in an ordered fashion across the data set. To test for an effect or interaction between two independent variables on a dependent variable, an ordinary or repeated-measures two-way ANOVA followed by Tukey's or Bonferroni multiple comparisons test was used. In addition, a Mann-Whitney *U*-test was used to compare two groups of data if they were not normally distributed. Finally, Fisher's exact test, which examines the association between two variables, was used to test for differences in frequency. Data were considered statistically different if the *P*-value was <0.05. In majority of cases, a two-tailed *P*-value was used; however, in a limited number of comparisons a one-tailed *P*-value was employed. The latter was the case when prior results indicated we could predict that, if there was to be a difference between the means of the two data sets, the difference would be in a particular direction.

## RESULTS

The bag cell neurons are located in two discrete clusters at the anterior portion of the abdominal ganglion, where the pleuro-abdominal connectives come down from the central ring portion of the nervous system (Kupfermann et al. 1966; Kupfermann and Kandel 1970) (Fig. 1A). The neurons fire in synchrony during an afterdischarge due to electrical synapses within and between the clusters (Blankenship and Haskins 1979; Haskins and Blankenship 1979). This was confirmed in the present study by making simultaneous intracellular recordings from two bag cell neurons in the same cluster (Fig. 1B).

Stimulation of the afferents in the connective with an extracellular electrode resulted in an afterdischarge, with simultaneous depolarization and action potential firing in both neurons. However, because the neurons are coupled to more than one partner, perhaps many more, the ability to study the electrical synapse in the intact cluster is limited. Thus we also performed experiments on dissociated cells in primary culture. Neurons were plated as pairs making soma-soma or, as shown in Fig. 1C, left, neurite-neurite contact. This allowed for a more direct examination of electrical coupling by simultaneous whole cell recording from two neurons with no additional neurons in contact. Figure 1C, right, presents a sample recording from two cultured bag cell neurons, where depolarizing current injection elicited action potentials in one neuron that in turn caused ETPs in the second neuron. Time in culture determined the probability of coupling, with ~80% of pairs forming detectable electrical synapses by 2–3 days in vitro but <10% of pairs coupling after 1 day in culture.

*Electrical synapse between cultured bag cell neurons is voltage independent.* Prior work has shown the gating of electrical synapses and gap junctions from a number of species to be either voltage dependent (Spray et al. 1979; Dykes et al. 2004) or voltage independent (Neyton and Trautmann 1985; Wildering and Janse 1992; White et al. 2004). To investigate this in bag cell neurons, pairs of electrically coupled cultured cells were whole cell voltage clamped with our regular, K<sup>+</sup>-aspartate-based intracellular saline in the pipettes and Na<sup>+</sup>-based nASW in the bath (Fig. 2B, inset). With the exception of certain electrotonic transmission and permeability experiments (see *Electrotonic signaling between cultured coupled bag cell neurons* and *Permeability of the cultured bag cell neuron electrical synapse*), all cultured bag cell neuron recordings used these salines. Both neurons were held at -60 mV and

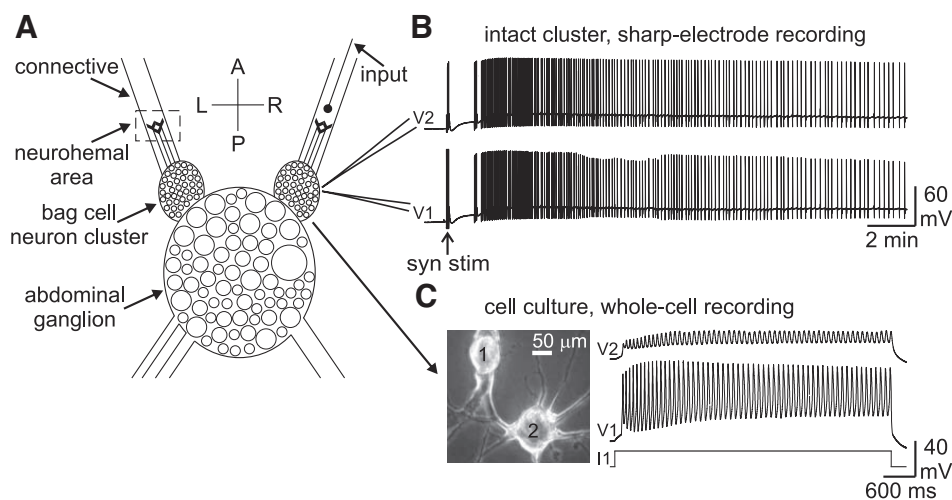


Fig. 1. Electrical coupling and synchronous firing in bag cell neurons. *A*: diagram of the bag cell neurons in the abdominal ganglion (dorsal view). The clusters sit at the insertion points of the pleuro-abdominal connectives, which descend from the rest of the central nervous system. The connectives house the terminals of the afferents that trigger the afterdischarge, as well as a neurohemal area where the bag cell neurons project axons into the sheath to secrete egg-laying hormone (dashed box). Inputs and neurohemal area are bilateral but are shown as singular for clarity. *B*: sharp-electrode current-clamp recording of 2 neurons in the intact bag cell neuron cluster from the abdominal ganglion. Shortly after extracellular stimulation of the synaptic input in the connective (syn stim; at arrow; 5 ms, 20 V at 5 Hz for 5 s), both neurons depolarize from resting potential ( $V_1 = -60$  mV;  $V_2 = -52$  mV) by ~20 mV and afterdischarge. Spiking during the afterdischarge is synchronous, with an initial fast phase followed by a slower phase of firing. This afterdischarge lasts just over 20 min but is truncated for display. Scale bars apply to both traces. *C*, left: a pair of bag cell neurons after 2 days in primary culture. The somata are numbered and contact between neurites is apparent in the bottom left corner of the photomicrograph. Right: whole cell current-clamp recording of electrically coupled cultured bag cell neurons in normal artificial sea water (nASW) with K<sup>+</sup>-aspartate-based intracellular saline in the pipettes. Both neurons are initially set at -60 mV with constant bias current; injection of depolarizing current (*I*; 1 nA, 5 s) into neuron 1 evokes action potentials ( $V_1$ ) that transfer to neuron 2 as electrotonic potentials (ETPs) ( $V_2$ ). Scale bars apply to both traces.

then one cell was stepped through a series of 10-mV square pulses from  $-90$  mV through to  $0$  mV in 200-ms intervals, while keeping the other cell at  $-60$  mV (Fig. 2A, *top* and *bottom middle*). Neurons were identified as *neuron 1* and *neuron 2*, with the protocol run using *neuron 1* as presynaptic (receiving voltage pulses) and *neuron 2* as postsynaptic (held at  $-60$  mV) and vice versa ( $n = 11$  pairs). In response to the step commands, the presynaptic neuron displayed membrane current that was linear near  $-90$  mV but then rectified outwardly in a time- and voltage-dependent manner closer to  $0$  mV, while the postsynaptic neuron presented a nearly instantaneous and completely linear current to all test pulses (Fig. 2A, *top middle* and *bottom*). The current in the postsynaptic neuron represented the junctional current, i.e., that current required to keep the cell voltage clamped at  $-60$  mV in the face of the potential difference across the junction created by a given test voltage in the presynaptic neuron. When the average steady-state postsynaptic current (junctional current) was plotted against the presynaptic voltage step, a linear current-voltage relationship was evident (Fig. 2B). This was the case regardless if either *neuron 1* or *neuron 2* received the voltage protocol as the presynaptic cell. Furthermore, in all 11 pairs, the junctional current did not rectify and was same magnitude when either *neuron 1* or *neuron 2* served in a presynaptic role.

Membrane conductance ( $G$  membrane) and junctional conductance ( $G$  junction) were obtained by dividing the steady-state presynaptic membrane current and junctional current (both measured within 20 ms of the end of the step) by the membrane driving force (test voltage  $-60$  mV) and the transjunctional voltage ( $-60$  mV  $-$  test voltage), respectively. As such, we treated the  $-60$ -mV holding potential as the reversal potential for both the membrane and junctional conductance. Plotting either of these derived variables on the ordinate and the test voltage on the abscissa provided  $G$  membrane vs. voltage (Fig. 2C) and  $G$  junction vs. voltage (Fig. 2D) curves. As expected from the membrane current data, the presynaptic membrane conductance had a linear portion, composed of leak

channels, from  $-90$  mV to  $-50$  mV, and a nonlinear portion, composed ostensibly of voltage-gated  $K^+$  channels from  $-40$  to  $0$  mV. The membrane conductance was largely the same for both cells in the pairs, with neither *neuron 1* nor *neuron 2* yielding significantly different conductances at a given command potential. Conversely, junctional conductance showed no sensitivity to transjunctional voltage, and was approximately equal ( $8-10$  nS) at all command potentials, with no significant difference between any of the test voltages. Consistent with the junctional current not rectifying, the junctional conductance was not different when the presynaptic cell was *neuron 1* or *neuron 2*.

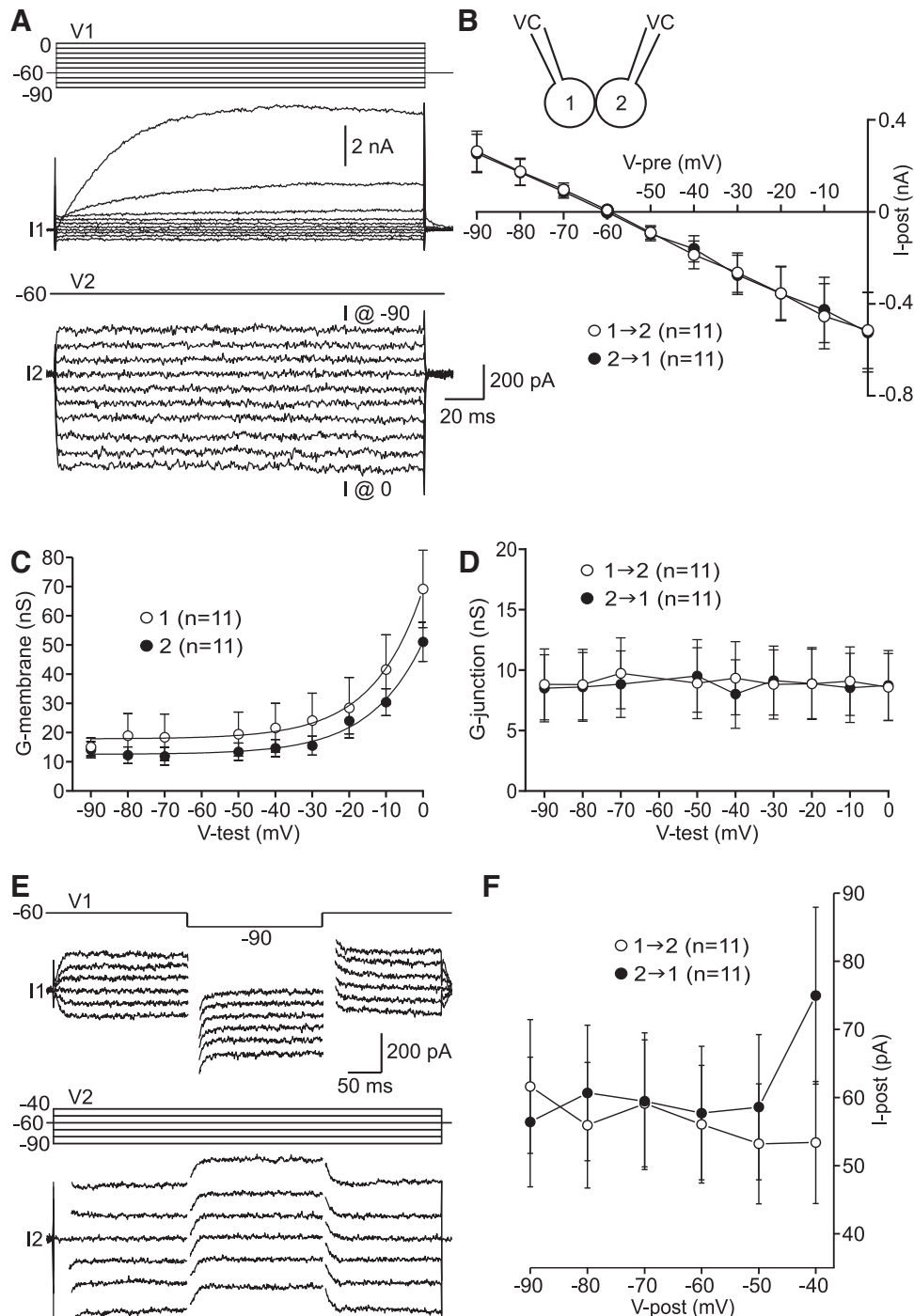
Having established that junctional current did not vary with presynaptic voltage, we next sought to determine if postsynaptic voltage could impact the behavior of the electrical synapse. Neuronal pairs ( $n = 11$ ) were again voltage clamped and the holding potential of the postsynaptic cell varied from  $-90$  to  $-40$  mV in 10-mV increments, while the presynaptic cell was stepped to  $-90$  mV for 200 ms to assay the junctional current (Fig. 2E, *top* and *bottom middle*). The change in postsynaptic current (junctional current) brought about by the test pulse to  $-90$  mV was similar regardless of the postsynaptic holding potential (Fig. 2E, *bottom*). A plot of junctional current against the postsynaptic membrane potential yielded a flat, linear relationship in all pairs studied (Fig. 2F). This lack of dependence of junctional current on inside-outside potential was apparent if either *neuron 1* or *neuron 2* acted as the postsynaptic cell.

*Cultured bag cell neuron electrical synapse is a low-pass filter.* A common feature of electrical coupling is that voltage signals are filtered in a low-pass manner when transferred from one cell to the other (Levitan et al. 1970; Getting 1974; Bennett 1977). This was examined in pairs of cultured bag cell neurons by voltage clamping the presynaptic neuron at  $-60$  mV while the postsynaptic neuron was also set to  $-60$  mV, but using bias current injection in current clamp (Fig. 3A, *left* and *right insets*). For each pair ( $n = 4$ ), *neuron 1* was treated as

Fig. 2. Electrical coupling between cultured bag cell neurons is independent of transjunctional and postsynaptic voltage. *A*: whole cell voltage-clamp recordings from a pair of electrically coupled cultured bag cell neurons in nASW dialyzed with  $K^+$ -aspartate-based intracellular saline. From a holding potential of  $-60$  mV for both *VI* and *V2*, stepping *VI* in 10-mV increments for 200 ms from  $-90$  mV to  $0$  mV elicits both presynaptic voltage-dependent membrane current (*I1*) in *neuron 1* and postsynaptic voltage-independent junctional current (*I2*) in *neuron 2*. The junctional currents evoked by hyperpolarizing and depolarizing pulses in *neuron 1* are seen in *neuron 2* as positive (e.g., *I* at  $-90$ ) and negative (e.g., *I* at  $0$ ) current, respectively. Scale bars apply to both traces. *B*: the steady-state postsynaptic current (*I-post*), i.e., junctional current resulting from presynaptic voltage steps (*V-pre*). Plotting the average current vs. the presynaptic voltage shows a linear, voltage-independent, and nonrectifying relationship in both directions. *Neuron 1* and *neuron 2* act reciprocally as pre- and postsynaptic ( $1 \rightarrow 2$  and  $2 \rightarrow 1$ ), depending on which is pulsed and which is maintained at  $-60$  mV. There is no significant interaction between direction and presynaptic voltage, as at any given voltage, the junctional current from *neuron 1* to *neuron 2* is not different from the current from *neuron 2* to *neuron 1* ( $F_{1,9} = 16.42$ ,  $P > 0.05$ , two-way repeated measures ANOVA;  $P > 0.05$  Bonferroni multiple comparisons test). In addition, both current-voltage relationships are essentially straight lines and have a significant linear trend such that the current increases in magnitude proportionally on either side of  $-60$  mV ( $1 \rightarrow 2$   $F_{1,8} = 76.3$ ,  $P < 0.0001$ , one-way ANOVA;  $2 \rightarrow 1$   $F_{1,8} = 71.5$ ,  $P < 0.0001$ , one-way ANOVA). *Inset*: recording configuration. *C* and *D*: membrane conductance ( $G$  membrane) or junctional conductance ( $G$  junction) plotted vs. test voltage. The  $G$ -membrane-voltage relationships of both bag cell neurons are well fit with a Boltzmann function (lines) and show outward rectification at membrane potentials more positive to  $-40$  mV, indicative of voltage dependence. However, at any given membrane potential, there is no difference between the conductance of *neuron 1* vs. *neuron 2* ( $F_{1,8} = 8.92$ ,  $P > 0.05$ , two-way repeated measures ANOVA;  $P > 0.05$  Bonferroni multiple comparisons test). Conversely, the junctional conductance is insensitive to voltage and essentially the same at all test potentials, with *neuron 1* ( $1 \rightarrow 2$ ) or *neuron 2* ( $2 \rightarrow 1$ ) serving as the presynaptic cell ( $F_{1,8} = 0.014$ ,  $P > 0.05$ , two-way repeated measures ANOVA;  $P > 0.05$  Bonferroni multiple comparisons test). Furthermore, the relationships between  $G$  junction and voltage are flat lines and fail to show a significant linear trend, in so much that the conductance does not appreciably change on either side of  $-60$  mV ( $1 \rightarrow 2$   $F_{1,7} = 0.007$ ,  $P > 0.05$ , one-way ANOVA;  $2 \rightarrow 1$   $F_{1,7} = 0.0004$ ,  $P > 0.05$ , one-way ANOVA). *E*: membrane (*I1*) and junctional (*I2*) currents in a different pair of voltage-clamped neurons where a test pulse from  $-60$  mV to  $-90$  mV is administered to the presynaptic cell (*VI*) while the postsynaptic cell (*V2*) is held between  $-40$  and  $-90$  mV. The junctional current is largely the same at all postsynaptic voltages. For clarity, capacitance artifacts have been removed from the current traces at the start and end of the presynaptic stimulus. Scale bars apply to both traces. *F*: current-voltage relationship between the postsynaptic membrane potential (*V-post*) and the postsynaptic current (*I-post*) elicited by the presynaptic test pulse. The postsynaptic current represents the junctional current and does not change appreciably while varying the postsynaptic voltage. This is the case when either *neuron 2* ( $1 \rightarrow 2$ ) or *neuron 1* ( $2 \rightarrow 1$ ) acts as the postsynaptic cell ( $F_{1,5} = 0.17$ ,  $P > 0.05$ , two-way repeated measures ANOVA;  $P > 0.05$  Bonferroni multiple comparisons test). Also, both relationships are essentially flat lines and lack a significant linear trend, where the current does not change from  $-90$  mV through to  $-40$  mV ( $1 \rightarrow 2$   $F_{1,4} = 0.92$ ,  $P > 0.05$ , one-way ANOVA;  $2 \rightarrow 1$   $F_{1,4} = 0.47$ ,  $P > 0.05$ , one-way ANOVA).

presynaptic and *neuron 2* as postsynaptic ( $1 \rightarrow 2$ ) and vice versa ( $2 \rightarrow 1$ ). The presynaptic neuron was stimulated with a train of 50, 85-ms hyperpolarizing voltage steps from  $-60$  to  $-90$  mV (Fig. 3B, top) at a frequency of 1, 5, or 10 Hz. The 85-ms step duration was long enough to produce a measurable postsynaptic response, while allowing for a stimulation frequency of up to 10 Hz. Normalizing the data by dividing all responses at a given frequency by the magnitude of the first response revealed little difference in the postsynaptic voltage change over time for the 1-Hz stimulus in either direction (Fig. 3A, white circles). However, for both the 5-Hz train (Fig. 3A, black circles) and particularly the 10-Hz train (Fig. 3A, grey circles),

the response quickly diminished with each subsequent step, up to the around the 10th pulse, after which no further change was observed. This was largely the same in both directions of stimulation. With the use of the 10th pulse as the assay point, the response of the postsynaptic neuron was found to be markedly smaller with faster stimulation frequency (Fig. 3B, bottom). The postsynaptic voltage change at all frequencies was normalized to the change observed at 1 Hz and plotted against the corresponding frequency (Fig. 3C). Indicative of low-pass filtering, when either *neuron 2* or *neuron 1* was the postsynaptic cell, the normalized attenuation was greater with increased presynaptic pulse frequency, more so for 1 vs. 10 Hz than 1 vs. 5 Hz.





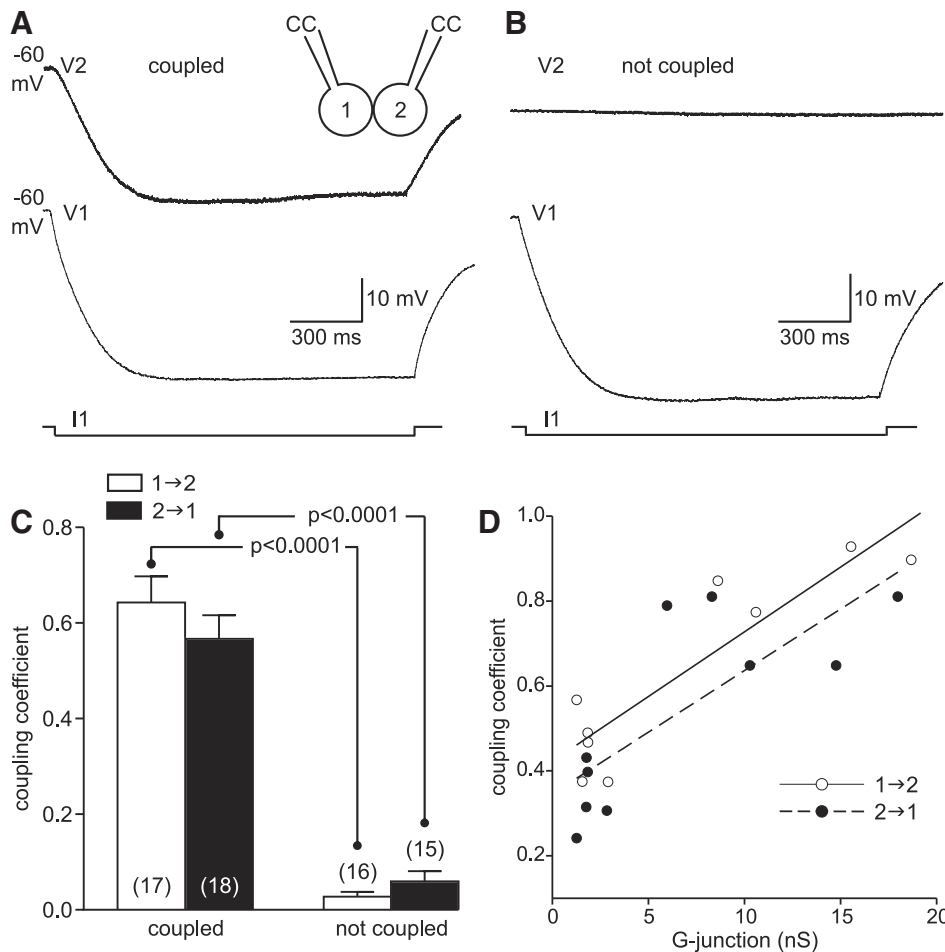


Fig. 4. Coupling coefficient between cultured bag cell neurons is large and linearly related to junctional current. *A* and *B*: whole cell current-clamp recordings from separate pairs of cultured bag cell neurons. The membrane potentials are first set to  $-60$  mV with bias current. *Inset*: recording configuration. *A*: response of coupled neurons (*V1* and *V2*) following a 1,500-ms injection of  $-250$  pA into *neuron 1* (*I1*). With a short delay, *neuron 2* follows *neuron 1*, leading to appreciable voltage transfer at steady-state (coupling coefficient 0.75). *B*: in a pair that are not coupled (cells are adjacent but not in physical contact), changing the presynaptic voltage has little postsynaptic impact. Scale bars apply to both traces in *A* or *B*. *C*: summary of coupling coefficient determined by the ratio of the steady-state pre- and postsynaptic response ( $V2/V1$  or  $V1/V2$ ) to presynaptic current (*I1* or *I2*). The low “coefficient” between not-coupled neurons is due to small, variations in voltage that most probably manifest as a result of high input resistance. Within coupled or not coupled groups, there is no statistical effect of whether *neuron 1* ( $1 \rightarrow 2$ ) or *neuron 2* ( $2 \rightarrow 1$ ) acts as the presynaptic cell ( $F_{14,42} = 1.2$ ,  $P > 0.05$ , two-way ordinary ANOVA) but a significant effect of whether or not the neurons are coupled ( $F_{3,42} = 60.7$ ,  $P < 0.0001$ , two-way ordinary ANOVA; Tukey’s multiple comparisons test). *D*: in a subset of coupled pairs, junctional conductance (determined as per Fig. 2*D*) is plotted against the corresponding coupling coefficient. Regression analysis shows a linear and positive correlation between coupling coefficient and junctional conductance ( $1 \rightarrow 2$   $R = 0.902$ ,  $R^2 = 0.81$ ,  $n = 9$ ,  $F_{1,7} = 30.4$ ,  $P < 0.001$ ;  $2 \rightarrow 1$   $R = 0.773$ ,  $R^2 = 0.60$ ,  $n = 10$ ,  $F_{1,8} = 11.8$ ,  $P < 0.01$ ).

on the ordinate yielded a linear and positive correlation (Fig. 4*D*). The higher the junctional conductance between a pair of neurons, the greater the coupling coefficients.

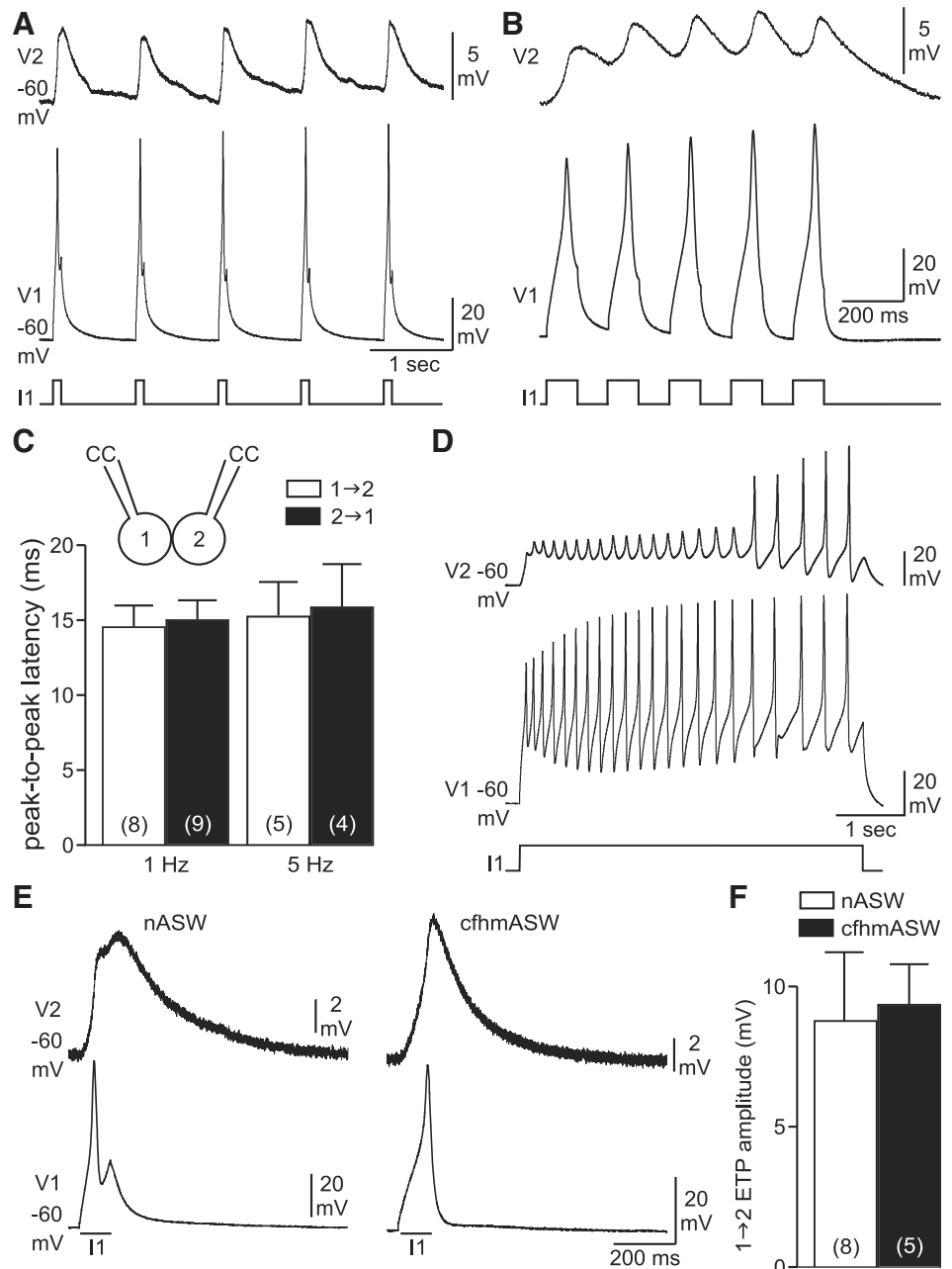
To evaluate electrotonic signaling, current-clamped pairs (Fig. 5*C*, *inset*) were set to  $-60$  mV and presynaptic action potentials elicited with five 100-ms, 750- to 1,000-pA depolarizing current steps at 1 or 5 Hz (Fig. 5, *A* and *B*, *bottom*). At both frequencies, a given presynaptic spike consistently produced a postsynaptic depolarizing ETP in a one-for-one relationship. For the 1-Hz train, there was near full recovery of postsynaptic voltage after each spike (Fig. 5*A*), while for the 5-Hz train, although still one-for-one, the action potentials resulted in ETPs that summated to keep the postsynaptic neuron somewhat depolarized throughout the train (Fig. 5*B*). Latency was rapid, with postsynaptic depolarization beginning early in the rising phase of the presynaptic action potential. Because of the ambiguity in precisely ascertaining when the postsynaptic response began, we quantitated latency by taking the time from the peak of the fifth action potential to the peak of the corresponding evoked ETP (Fig. 5*C*). This yielded an apparent latency of  $\sim 15$  ms that was not significantly different at either 1 or 5 Hz, regardless if *neuron 1* ( $n = 8$  or 5) or *neuron 2* ( $n = 9$  or 4) was the presynaptic cell.

Despite large coupling coefficients, individual ETPs were typically modest in amplitude, likely because of the filtering effect of the synapse. As such, individual presynaptic action potentials from  $-60$  mV provoked postsynaptic action poten-

tials in less than a third of pairs ( $n = 4$  out of 14). However, during the afterdischarge, bag cell neurons typically depolarize to between  $-40$  and  $-30$  mV (Kupfermann and Kandel 1970; Brown et al. 1989); thus, rather than being depolarized by short current pulses as in Fig. 5, *A* or *B*, the presynaptic neuron was tonically depolarized to fire a burst of action potentials ( $n = 22$ ; Fig. 5*D*). From a resting potential of  $-60$  mV for both cells, delivering a 5-s, 1-nA positive current pulse to *neuron 1* caused an approximately  $-30$  mV depolarization and continuous spiking, which transferred to *neuron 2* as both concomitant depolarization and ETPs, that in nearly half of pairs ( $n = 10$  of 22) induced postsynaptic action potentials.

Communication between pairs of bag cell neurons is consistent with electrical signaling; even so, there is evidence that, in addition to egg-laying hormone, these cells also secrete  $\alpha$ -,  $\beta$ -, and  $\gamma$ -bag cell peptides, which can depolarize bag cell neurons when applied exogenously (Loechner and Kaczmarek 1994; Hatcher and Sweedler 2008). To rule out the possibility that the ETP contained a chemical component, paired cultured bag cell neurons were bathed in  $\text{Ca}^{2+}$ -free/high- $\text{Mg}^{2+}$  ASW (0 mM  $\text{Ca}^{2+}$ , 66 mM  $\text{Mg}^{2+}$ ), and spikes initiated in *neuron 1* from  $-60$  mV with a 100-ms, 1-nA depolarizing current step ( $n = 5$  pairs). Without extracellular  $\text{Ca}^{2+}$ , the onset of the ETP still occurred before the peak of the presynaptic action potential (Fig. 5*E*, *right*), and the shape of the ETP was not dramatically altered compared with that produced in the presence of  $\text{Ca}^{2+}$  (Fig. 5*E*, *left*). The amplitude of the ETP in

Fig. 5. Cultured bag cell neuron electrical synapse transmits excitatory information. *A* and *B*: ETPs measured between 2 different pairs of cultured coupled bag cell neurons in nASW with  $K^+$ -aspartate-based intracellular saline in the pipettes and initially whole cell current clamped to  $-60$  mV. Evoking action potentials (*V1*) in *neuron 1* with 100-ms, 750-pA current injections (*I1*) at 1 Hz (*A*) or 5 Hz (*B*) reliably elicits ETPs in *neuron 2* (*V2*). The ETP during 1-Hz stimulation fully decays between presynaptic action potentials; however, summation is apparent during the 5-Hz input. Time base, in *A* and *B*, respectively, applies to both traces. *C*: summary data for latency from action potential peak to ETP peak. The delay is essentially the same at 1 Hz and 5 Hz, with no significant effect of the direction of coupling ( $1 \rightarrow 2$  or  $2 \rightarrow 1$ ;  $F_{3,9} = 1.9$ ,  $P > 0.05$ , two-way ordinary ANOVA) or the frequency of stimulation (1 or 5 Hz;  $F_{3,9} = 0.64$ ,  $P > 0.05$ , two-way ordinary ANOVA). *Inset*: recording configuration. *D*: delivering a 5-s, 1-nA current to *neuron 1* (*I1*) evokes a train of action potentials (*V1*) that initially transfers to *neuron 2* as ETPs, along with the steady-state depolarization, followed by genuine postsynaptic spikes (*V2*). Representative of 10 experiments. Time base applies to both traces. *E*: 2 different pairs of coupled bag cell neurons bathed in  $Ca^{2+}$ -containing nASW or  $Ca^{2+}$ -free/high- $Mg^{2+}$  ASW (cfhmASW). *Left*: when extracellular  $Ca^{2+}$  is present, eliciting an action potential from *neuron 1* (*V1*) with a 100-ms, 1-nA current (*I1*; at bar) produces an ETP in *neuron 2* (*V2*). The postsynaptic voltage exhibits a second peak on account of an aborted presynaptic spike starting just as the current injection ends. *Right*: in the absence of  $Ca^{2+}$ , an action potential in *neuron 1* provokes an ETP of similar magnitude in *neuron 2*. Note that in cfhmASW the upstroke of the action potential is less steep, which is often the case given the  $Ca^{2+}$  dependence of the bag cell neuron spike. In both salines, the ETP begins during the rising phase of the presynaptic action potential. *Top traces* both scaled the same. Time base applies to all traces. *F*: summary data of the ETP amplitude in the presence (nASW) or absence (cfhmASW)  $Ca^{2+}$  in the bath demonstrates no difference between the 2 conditions (one-tailed, unpaired Student's *t*-test). The nASW data are taken from the first ETP in the 1-Hz stimulus-train experiments shown in *A* and *C*.



$Ca^{2+}$ -free/high- $Mg^{2+}$  ASW was not statistically different from that evoked in nASW (Fig. 5F).

**Coupled cultured bag cell neurons fire synchronously.** The afterdischarge presents as synchronous neuronal firing (Kupfermann and Kandel 1970; Blankenship and Haskins 1979). To examine how the electrical synapse could shape such activity, whole cell current clamp was used to record from pairs of cultured bag cell neurons that were either coupled or not coupled (Fig. 6E, inset). Again, not-coupled pairs consisted of neurons not making contact or the electrical synapse not materializing despite contact. Continuous action potential firing was elicited in *neuron 1* and *neuron 2* by simultaneously injecting both cells with a 1-nA, 5-s depolarizing current step. When cells from coupled pairs ( $n = 10$ ) were made to spike in this manner, the action potentials from *neuron 1* and *neuron 2*

were phase locked with a high degree of adherence (Fig. 6A, expanded inset). Not-coupled pairs ( $n = 7$ ) showed that action potentials from *neuron 1* and *neuron 2* were independent and mostly out of phase, with any concurrent firing being coincidental (Fig. 6B, expanded inset). A pair was considered synchronous if the firing in both neurons consistently occurred at the same time or if one cell preceded the other by a short, fixed time period. Synchrony was quantitated using cross-correlation to compare the regularity of the action potential waveforms of both cells. Specifically, the signal from *neuron 1* was shifted, both forward and back, along the signal from *neuron 2* to produce a cross-correlation function estimate, which was then plotted as a cross-correlogram. Coupled pairs furnished cross-correlograms with relatively large estimates ( $\geq 0.75$ ) situated near a lag of zero (absolute correlation) on the abscissa (Fig.

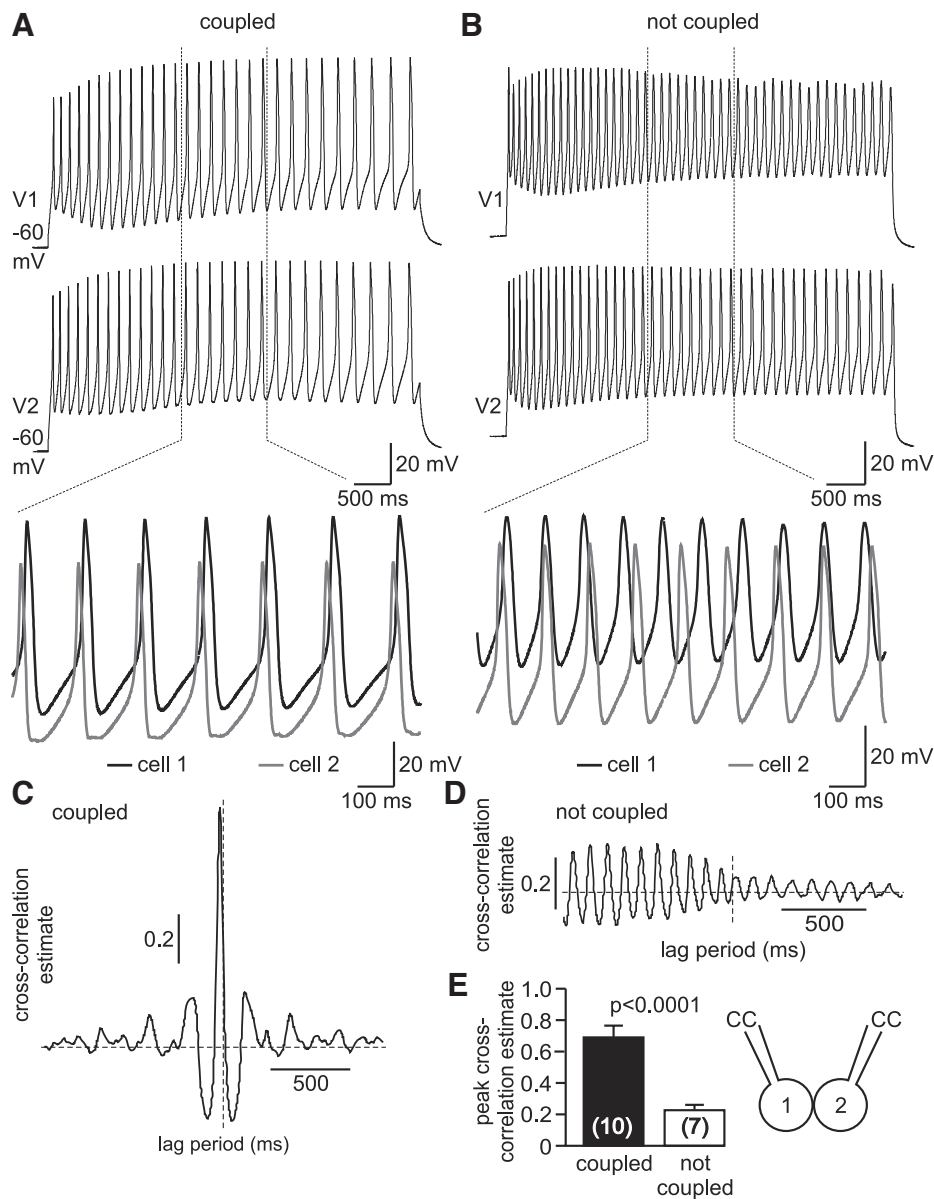


Fig. 6. Action potential synchrony between electrically coupled cultured bag cell neurons. *A* and *B*: 2, separate pairs of cultured bag cell neurons initially current clamped to  $-60$  mV in nASW and dialyzed with  $K^+$ -aspartate-based intracellular saline. In either the coupled (*A*) or not-coupled (*B*) pair, cells are induced to fire continuously by 5-s, 1-nA current injections into both neurons (*V1* and *V2*). Scale bars apply to both traces in *A* or *B*. *Bottom*: mid-sweep expansions (indicated by the dashed lines) showing the action potentials of *neuron 1* (black trace) and *neuron 2* (grey trace). In the coupled pair, the waveforms synchronize, with *neuron 2* always spiking just before *neuron 1*. However, the not-coupled pair lacks synchronization and the spikes go in and out of phase over the course of the sweep. *C* and *D*: cross-correlograms describing the extent to which the 2 traces from *A* or *B* match. Shifting the data from *neuron 1* along that of *neuron 2* by 1,000 lags in both directions generates the cross-correlation estimate plotted on the ordinate. Intersection of the dashed lines at zero indicates perfect correlation. *C*: consistent with strong synchrony of firing, the coupled neurons present a high cross-correlation estimate ( $\sim 0.95$ ) just to the left of the intersection. *D*, the not-coupled pair fails to display a sizeable cross-correlation estimate over any of the lag period. *E*: summary data indicating a significantly higher peak cross-correlation estimate during action potential firing of coupled neurons compared with not-coupled neurons (two-tailed, unpaired Student's *t*-test). *Inset*: recording configuration.

6C), whereas not-coupled pairs rendered relatively small estimates ( $\leq 0.3$ ) that consistently did not fall near zero lag (Fig. 6D). The peak cross-correlation estimates were higher for coupled pairs vs. not-coupled pairs, and this difference reached significance (Fig. 6E).

**Permeability of the cultured bag cell neuron electrical synapse.** Passage of dyes or various ionic species between coupled cells has often been used to define permeability characteristics of electrical synapses (Payton et al. 1969; Stewart 1978; Peinado et al. 1993). Kaczmarek et al. (1979) reported occasional dye coupling using Lucifer Yellow injections both in the intact cluster and between cultured bag cell neurons. We expanded on this by introducing either sulforhodamine or carboxyfluorescein (both dissolved in regular intracellular saline) through the whole cell pipette under voltage clamp at  $-60$  mV into one of the two cells from a pair of cultured bag cell neurons. In most cases, the second cell was also whole cell voltage clamped at  $-60$  mV, but with a dye-free pipette, and coupling was confirmed

under voltage clamp. Staining of one neuron for  $\sim 30$  min did not result in appreciable dye transfer when either sulforhodamine ( $n = 4$  at 0.1% wt/vol and  $n = 3$  at 0.5%) or carboxyfluorescein ( $n = 5$  at 0.1% and  $n = 3$  at 0.5%) was used (Fig. 7, *A* and *B*). This was observed both at the end of the recording period or if the electrodes were taken off the neurons and the dish kept overnight in the incubator ( $n = 2$  for sulforhodamine and  $n = 2$  for carboxyfluorescein). As an alternative to whole cell dye loading, we also sharp-electrode current clamp to ionophoretically injected biocytin ( $n = 6$ ) into one of the cells from a pair of cultured bag cell neurons. Following an overnight period in the incubator, pairs were exposed to streptavidin-Alexa Fluor 488 conjugate. The high-affinity binding of streptavidin to biocytin allows for fluorescence-based localization of the tracer subsequent to any diffusion (Heitzmann and Richards 1974; Horikawa and Armstrong 1988). Nevertheless, biocytin was also not detected in the cell contacting the injected neuron (Fig. 7C).



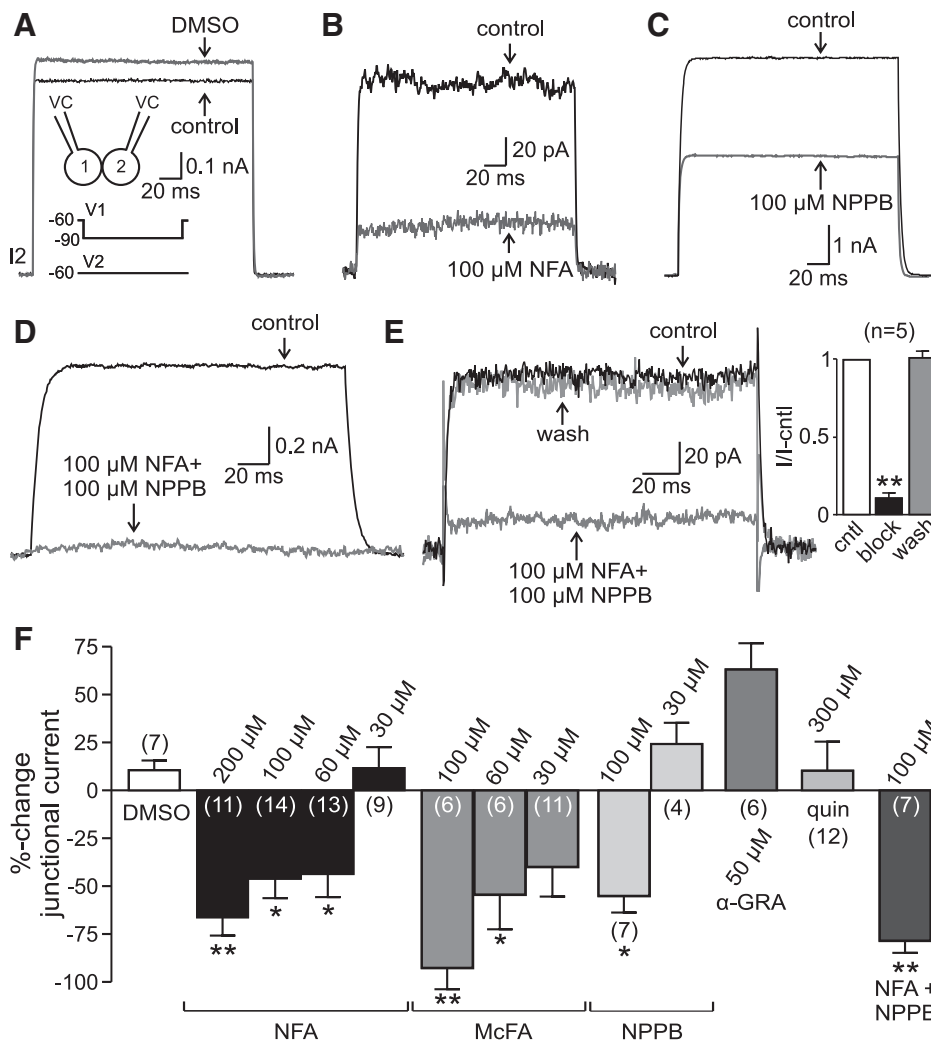


Fig. 8. Select gap junction blockers attenuate electrical coupling between cultured bag cell neurons. *A*: junctional current recorded in *neuron 2* from a coupled cultured bag cell neuron pair dialyzed with  $K^+$ -aspartate-based intracellular saline under whole cell voltage clamp in nASW (*top inset*; VC). From a holding potential of  $-60$  mV for both *V1* and *V2*, a test pulse to  $-90$  mV in *neuron 1*, while continuing to hold *neuron 2* at  $-60$  mV (*bottom inset*), evokes junctional current (*I2*). Compared with control, there is a slight increase in junctional current 10 min after bath application of DMSO. *B–D*: introducing  $100 \mu\text{M}$  of either of the gap junction blockers niflumic acid (NFA; *B*) or 5-nitro-2-(3-phenylpropylamino)benzoic acid (NPPB; *C*) markedly decreases junctional current. Moreover, when  $100 \mu\text{M}$  of each of these blockers are delivered together, coupling is almost completely eliminated (*D*). *E*: one-and-a-half min of perfusing the NFA plus NPPB cocktail over a pair of coupled bag cell neurons reduces the junctional current. This fully recovers back to control levels after 5 min of wash with nASW. *Inset*: summary data show the extent of block and reversibility of the combination of NFA and NPPB ( $F_{2,12} = 268.6$ ,  $P < 0.0001$ , one-way ANOVA;  $**P < 0.01$ , Dunnett multiple comparisons test). *F*: summary graph of percentage change from control in junctional current subsequent to adding vehicle or drug. Compared with DMSO, NFA ( $30$  to  $200 \mu\text{M}$ ), meclofenamic acid (McFA;  $30$ – $100 \mu\text{M}$ ), and NPPB ( $30$  and  $100 \mu\text{M}$ ) significantly inhibit junctional current in a dose-dependent manner. However,  $50 \mu\text{M}$   $\alpha$ -glycyrrhetic acid ( $\alpha$ -GRA) and  $300 \mu\text{M}$  quinine (quin) do not; in fact,  $\alpha$ -GRA may enhance coupling. In addition, a cocktail of NFA and NPPB ( $100 \mu\text{M}$  each) results in a block that is more effective than either agent alone ( $F_{12,100} = 10.3$ ,  $P < 0.0001$ , one-way ANOVA;  $*P < 0.05$ ,  $**P < 0.01$ , Dunnett multiple comparisons test).

min (Fig. 8*E*), which was fully reversible after 5–10 min following the return of the perfusate to nASW (Fig. 8*E*, *inset*). The effects of NFA or NPPB, as well as another arylaminobenzoate, meclofenamic acid (McFA), were concentration dependent, with  $30$  or  $60 \mu\text{M}$  having less or no impact compared with  $100$  or  $200 \mu\text{M}$  (Fig. 8*F*).

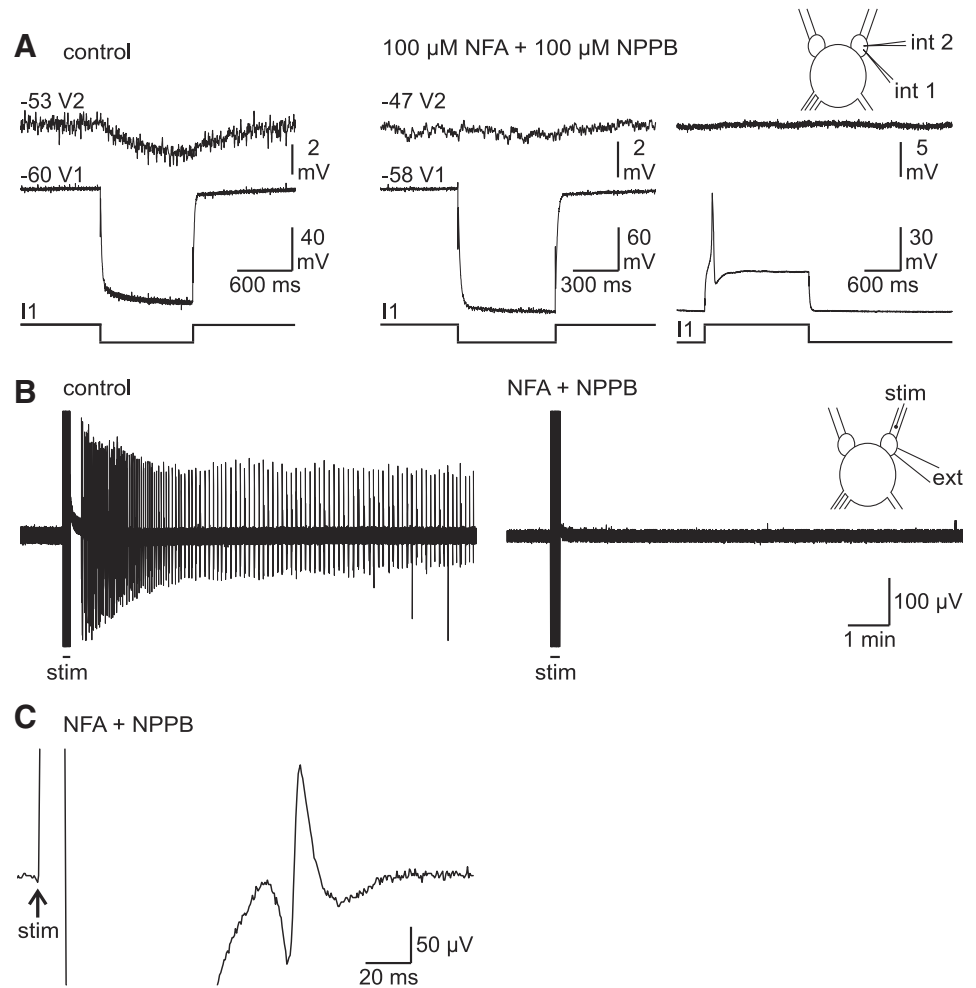
Neither NFA nor NPPB at  $100 \mu\text{M}$  had any obvious consequence on membrane conductance (measured in *neuron 1* from the steady-state current during a  $100$ -ms step to  $-10$  mV from a holding potential of  $-60$  mV); moreover, NFA and NPPB in combination altered the membrane conductance by only  $-6.1 \pm 16.9\%$  ( $n = 6$ ). However,  $100$  or  $200 \mu\text{M}$  McFA often produced up to an  $\sim 80\%$  increase in membrane conductance; as such, despite being an effective blocker, this drug was not pursued further. Two other gap junction blockers,  $50 \mu\text{M}$   $18\text{-}\alpha$ -glycyrrhetic acid ( $n = 6$ ) and  $300 \mu\text{M}$  quinine ( $n = 12$ ), did not inhibit the junctional current (Fig. 8*F*). Finally, as mentioned in the MATERIALS AND METHODS, we were unable to successfully dissolve and test carboxelone, a glycyrrhetic acid-derivative widely used to block gap junctions (Davidson and Baumgarten 1988; Juszczak and Swiergiel 2009).

Both electrical coupling and the afterdischarge in the intact bag cell neuron cluster are suppressed by gap junction blockers. To investigate the role of electrical coupling in afterdischarge generation, abdominal ganglia were excised,

and intra- or extracellular voltage recordings were made from bag cell neurons in the intact cluster or the entire cluster itself, bathed in control nASW vs. gap junction block with NFA and NPPB. Initially, pairs of bag cell neurons from the same cluster were impaled with sharp electrodes to monitor membrane potential (Fig. 9*A*, *inset*). Coupling was detected in clusters from five control ganglia; strong hyperpolarization of one neuron, by negative current injection, consistently resulted in a small, but detectable hyperpolarization in the second neuron, and vice versa (Fig. 9*A*, *left*). In five other ganglia, paired recordings from clusters showed that the postsynaptic hyperpolarization was attenuated by a 10- to 15-min incubation in the  $100 \mu\text{M}$  NFA and  $100 \mu\text{M}$  NPPB cocktail (Fig. 9*A*, *middle*). The coupling coefficient dropped significantly from  $0.0143 \pm 0.0046$  ( $n = 5$ ) in control to  $0.0026 \pm 0.0024$  in NFA plus NPPB ( $n = 5$ ;  $P < 0.03$ , one-tailed unpaired Student's *t*-test). Nevertheless, neurons remained excitable in NFA plus NPPB, with depolarizing current injection readily evoking action potentials, although these did not produce appreciable ETPs in the postsynaptic neuron (Fig. 9*A*, *right*).

The intracellular data suggested that electrical coupling is present in our preparations; thus we next looked at the afterdischarge itself by using suction electrodes to make both extracellular recordings from the intact bag cell neuron

Fig. 9. Gap junction blockers attenuate electrical coupling and alter afterdischarge generation in the intact bag cell neuron cluster. **A:** paired, intracellular (*int 1* and *int 2*) sharp-electrode current-clamp recordings (*inset*) of bag cell neurons from the intact cluster in abdominal ganglia bathed with nASW. **Left:** control injection of a 4-nA hyperpolarizing current step (*I1*) into one neuron (*V1*) causes a large hyperpolarization that transfers to a second neuron (*V2*) as a small, concomitant change in membrane potential (coupling coefficient 0.02). **Middle:** treating a different cluster for 10 min with 100  $\mu$ M of both NFA and NPPB lessens the response in the second neuron (*V2*) to hyperpolarization (*I1*) of the first neuron (*V1*). **Right:** also in NFA plus NPPB, evoking a spike in the first neuron with a 2-nA depolarizing current step fails to cause an ETP in the second neuron. Resting potentials (with no bias current) are given at the start of each trace. Time base applies to both traces in each panel. **B:** ensemble extracellular recordings (*ext*) from the intact bag cell neuron cluster following stimulation of the corresponding pleuroabdominal connective (*stim*) in the abdominal ganglia (*inset*) bathed with nASW. **Left:** exciting the synaptic input (*stim*; at bar; 5 ms, 20 V at 5 Hz for 10 s) under control conditions elicits a typical afterdischarge with a fast- and slow-phase. This afterdischarge lasts 24 min, but is truncated at 9 min for display. **Right:** a 10-min incubation of a different preparation with NFA and NPPB renders stimulation of the connective ineffective at provoking an afterdischarge. **C:** in the presence of NFA and NPPB, the intact cluster is still excitable, as a individual stimulus input (at arrow; 20 V) evokes a compound extracellular action potential. Stimulus artifact truncated at top and bottom for clarity.



cluster in the abdominal ganglion and stimulate the synaptic input descending via the pleuroabdominal connective (Fig. 9B, *inset*). These recordings were ensemble and represented the activity of the entire cluster (Kupfermann and Kandel 1970; Dudek and Blankenship 1977). In all five control preparations, afferent activation triggered an afterdischarge, with a characteristic 1- to 2-min fast phase of firing at the start, followed by a 20- to 30-min slow-phase, and an average duration of  $24.5 \pm 2.3$  min (Fig. 9B, *left*). However, in five other ganglia treated with NFA plus NPPB, four clusters failed to display an afterdischarge (Fig. 9B, *right*), and only one cluster actually fired a normal, prolonged burst following synaptic input. As such, the difference in the frequency of afterdischarge occurrence between control ganglia and ganglia incubated in the mixture of NFA and NPPB was significant ( $P < 0.04$ , two-tailed Fisher's exact test). Furthermore, the average duration of the afterdischarge under gap junction block,  $6.1 \pm 6.1$  min, was also significantly different from control ( $P < 0.05$ , one-tailed Mann-Whitney *U*-test). The lack of afterdischarges in the presence of gap junction blockers was not due to a failure of the input to provoke synaptic responses or action potentials in the bag cell neurons. Figure 9C shows that pleuroabdominal connective stimulation was still capable of eliciting an action potential in an intact cluster bathed with NFA plus NPPB.

## DISCUSSION

Electrical synapses allow for current to pass directly from cell to cell, thus providing a means for the membrane potential of a neuron to immediately and reliably influence that of neighbouring neurons (Bennett and Zulkun 2004; McCracken and Roberts 2006). The characteristics of bag cell neuron communication are consistent with an electrical synapse, presumably mediated by gap junctions. In the intact cluster, this would promote firing synchrony during the afterdischarge, leading to en masse secretion of egg-laying hormone and reproduction (Dudek et al. 1979; Stuart et al. 1980; Michel and Wayne 2002; Hatcher and Sweedler 2008).

Cultured bag cell neurons appear to form electrical, rather than chemical, synapses. In voltage clamp, presynaptic depolarization or hyperpolarization results in a near-simultaneous flow of current from pre to postsynaptic neuron. In current clamp, presynaptic depolarization or hyperpolarization causes a concomitant change in postsynaptic membrane potential. Chemical transmission would present  $\text{Ca}^{2+}$  sensitivity, and the change in postsynaptic voltage or current would occur at a fixed latency following the presynaptic stimulus (Katz and Miledi 1967; Berry and Pentreath, 1976; Llinas et al. 1981). However, as expected for electrical transmission, the amplitude and time course of the ETP are not altered when extracellular  $\text{Ca}^{2+}$  is removed; furthermore, the onset of the ETP occurs before the peak of the presynaptic action potential (Bennett

1977, 2000). There are two prior studies involving cultured bag cell neuron electrical synapses (Kaczmarek et al. 1979; Lin and Levitan 1987). Although less quantitative than the present study, they do show presynaptic hyperpolarization and action potentials eliciting postsynaptic hyperpolarization and ETPs/spikes, respectively.

The pharmacological profile of the bag cell neuron junctional current also points to an electrical synapse. All of the arylaminobenzoates inhibited the junctional current, with a combination of NFA and NPPB being the most effective, including blocking electrotonic transmission in the intact cluster. These drugs inhibit electrical synapses between hepatoma or neuroblastoma cells transfected with various connexin genes, as well as horizontal cells in the retina and connexin hemichannels in oocytes (Harks et al. 2001; Eskandari et al. 2002; Srinivas and Spray 2003; Pan et al. 2007). Long-chain alcohols, like heptanol or octanol, also block electrical transmission in many species (Johnston et al. 1980; Juszczak and Swiergiel 2009). However, we did not test them because earlier reports indicated they were ineffective on coupled L14 *Aplysia* ink motor neurons in situ as well as pairs of coupled *Aplysia* buccal, cerebral, or pleural neurons in vitro (Carew and Kandel 1977; Bodmer et al. 1988; Carrow and Levitan 1989). Those results, along with our finding that neither glycyrrhetic acid nor quinine blocks the bag cell neuron electrical synapse, may suggest that *Aplysia* gap junction proteins (Apl-innexins) are distinct from innexins in *Drosophila*, crayfish, or the pulmonate mollusk *Limax*, which are inhibited by alcohols or glycyrrhetic acid (Johnston et al. 1980; Cao and Nitabach 2008; Ermentrout et al. 2004). The original *Aplysia* neuronal transcriptome yielded nine predicted Apl-innexin genes (Moroz et al. 2006), while our initial PCR-based cloning indicates 20 full-length Apl-innexins (Carter and Magoski 2014). Like *Drosophila*, leech, and the gymnosomatan mollusk *Clione*, all Apl-innexins have four predicted transmembrane domains, two Cys in both extracellular loops, thought to be critical for hemichannel interaction, and the Pro-X-X-X-Trp motif in the second transmembrane domain (Phelan et al. 2008). However, only around a third have consensus for the so-called insect innexin signature sequence Tyr-Tyr-Gln-Trp-Val. Thus the molecular substrate for gap junctions is present, although differences in protein structure or assembly could account for the distinct pharmacological and biophysical profile of the bag cell neuron electrical synapse.

Despite dye coupling often being used as a criterion for the presence of electrical synapses (Stewart 1978; Peinado et al. 1993), we did not detect transfer of either of the polar dyes sulforhodamine or carboxyfluorescein, as well as the weakly charged tracer biocytin. The latter is somewhat unexpected, given that biocytin usually crosses gap junctions when other tracers fail (Ewadinger et al. 1994). Dye coupling is also not observed between *Aplysia* L14 neurons (Bodmer et al. 1988) or *Caenorhabditis* myocytes (Liu et al. 2006), although other invertebrate neurons dye couple, including those from the pulmonate mollusks *Lymnaea* and *Helisoma* (Murphy et al. 1983; Ewadinger et al. 1994), as well as crayfish (Payton et al. 1969) and leech (Fan et al. 2005). One confounding factor is that any dye that transferred from one neuron to the other may have been diluted by the regular pipette solution used to recorded from the second cell. That stated, the dye certainly would have had a chance to diffuse across the electrical

synapse without interference in those pairs incubated overnight.

Our postsynaptic K<sup>+</sup> channel block experiments imply that Cs<sup>+</sup>, but not TEA, permeates the bag cell neuron gap junction. The ionic radius of TEA is two to three times that of Cs<sup>+</sup>, which in turn is only slightly larger than K<sup>+</sup> (Hille 2001), the likely dominant charge carrier under normal circumstances. Curiously, Bodmer et al. (1988) demonstrated TEA permeability between L14 neurons in situ and in culture. This discrepancy may be due to differences in expression of specific Apl-innexins in bag cell vs. L14 neurons. Furthermore, Bodmer et al. (1988) found that TEA readily transferred between L14 pairs in situ (where the junctional conductance was hundreds of nS) but had varying success in vitro, with some pairs presenting little-to-no TEA transfer, particularly when the conductance was in the 10-nS range. Given that the mean junctional conductance for cultured bag cell neurons is <10 nS, the permeability pathway may be insufficient for the larger TEA compared with the smaller Cs<sup>+</sup> ion. Overall, compared with other connexins and innexins (Deschênes and Bennett 1974; Verselis et al. 1986; Beblo and Veenstra 1997), bag cell neuron junctional channels appear to be more restrictive.

The junctional current between cultured bag cell neurons is independent of both junctional voltage and the postsynaptic membrane potential. This is also the case for coupled L14, coupled B30/B63/B65, and paired cultured buccal, cerebral, or pleural *Aplysia* neurons (Bodmer et al. 1988; Carrow and Levitan 1989; Sieling et al. 2014) as well as identified visceral-parietal neurons from *Lymnaea* (Wildering and Janse 1992). Many vertebrate gap junctions have some form of voltage dependence (Spray et al. 1979; Bukauskas and Verselis 2004), as do some leech innexins (Dykes et al. 2004) and electrical synapses in the midge *Chironomus* (Obaid et al. 1983). However, closure of certain connexins, such as Cx26, does not occur until the junctional voltage is altered by >75 mV. The presynaptic voltage changes used in the present study are at the physiological limits of resting potential (−90 to 0 mV); yet, if these were extended to non-physiological voltages, the junctional current may display voltage dependence. The bag cell neuron electrical synapse also does not rectify, as all assays consistently show current or voltage transmitting equally well from *neuron 1* to *neuron 2* and vice versa. Rectification is absent from most coupled molluscan neurons, including *Aplysia* (Bodmer et al. 1988; Carrow and Levitan 1989), *Lymnaea* (De Vlieger et al. 1980; Wildering et al. 1991), and the nudibranch *Tritonia* (Getting 1974). There are cases of apparent rectifying electrical synapses in *Aplysia* (Waziri 1969; Wu et al. 2014), but these appear to be asymmetrically coupled neurons, where any directional inequality in coupling coefficient is due to differences in capacitance or input resistance of one of the neurons, rather than genuine direction differences in junctional conductance.

Although the bag cell neuron electrical synapse is very reliable, with no observed failures either in culture or the intact cluster, the low-pass filter function does limit transmission. This is inherent to most gap junctions and manifests as a reduction in any presynaptic voltage change as it passes to the postsynaptic neuron, particularly for rapid or higher frequency signals (Bennett 1977, 2000). In bag cell neurons, the time needed for charging the postsynaptic capacitance draws out and dampens the ETP; hence a 70–90 mV magnitude presyn-

aptic action potential renders an  $\sim 10$  mV ETP with a peak-to-peak latency of  $\sim 15$  ms. However, at steady state, low-pass filtering is less consequential, and the 20- to 30-mV chronic depolarization associated with the afterdischarge likely transfers effectively between neurons (Kupfermann and Kandel 1970; Brown et al. 1989). From these depolarized membrane potentials, spiking in one neuron would tend to evoke spiking in a coupled partner.

Firing synchrony is a key feature of the afterdischarge, and since early descriptions of bag cell neuron function, it has been asserted that electrical coupling underlies this phenomenon (Kupfermann and Kandel 1970; Blankenship and Haskins 1979). We find that when paired cultured bag cell neurons are made to spike simultaneously with dual current injection, their firing is highly synchronized, but only if they are electrically coupled and not if the gap junction is absent. Moreover, the gap junction blockers NFA and NPPB (Harks et al. 2001; Srinivas and Spray 2003) largely prevent afterdischarge generation in the intact bag cell neuron cluster. However, despite our observing essentially no side-effects for NFA and NPPB on whole cell conductance in vitro, or the ability of either current injection or pleuro-abdominal connective stimulation to trigger action potentials in situ, we cannot rule out the possibility that these drugs may act on nongap junction targets in a manner analogous to what has been described elsewhere. For example, there are reports of arylaminobenzoates, more so for flufenamic acid (which we did not employ here) and McFA, rather than NFA or NPPB, opening  $K^+$  channels, releasing intracellular  $Ca^{2+}$ , or blocking various channels (Gogelein et al. 1990; White and Alywin 1990; Poronnik et al. 1992; Takahira et al. 2005; Gardam et al. 2008).

The voltage-independent nature of the bag cell neuron electrical synapse translates into the junction being open at rest, which would allow current to spread through the network from neurons receiving excitatory acetylcholine synapses (White and Magoski 2012). Spatial spread of excitation within the cluster was postulated by Brown and Mayeri (1989), who envisaged electrical coupling acting as part of a positive-feedback mechanism promoting the afterdischarge. Similarly, electrical synapses are required to distribute synaptic depolarization and drive synchronous afterdischarges in prey capture motor neurons of *Clione* (Norekian 1999), while electrical synapses mediate regenerative excitation of trigger-group neurons that burst simultaneously to control swimming in *Tritonia* (Getting and Willows 1974). If the cholinergic input that initiates the afterdischarge is limited to a select few bag cell neurons (White and Magoski 2012), then blocking gap junctions may occlude the spread of excitation and, as we saw for most preparations, result in a paucity of firing.

Coupling in the intact bag cell neuron cluster is quite low, with a coupling coefficient of  $\sim 0.015$ , which is about fivefold greater than the  $\sim 0.0075$  value reported by Blankenship and Haskins (1979) for *A. dactylorella*. The difference between culture and the intact cluster likely reflects electrotonically remote gap junctions in the former, due to the electrical synapses being far away from the soma and multipartner coupling effectively reducing the input resistance of any given neuron (Kaczmarek et al. 1978; Blankenship and Haskins 1979). Nevertheless, strong coupling is not necessarily required for synchrony; similar to what we report, various networks of rat cortical or thalamic neurons show synchrony

despite presenting very low coupling coefficients (Gibson et al. 1999; Traub et al. 2001; Landisman et al. 2002). Bag cell neuron secretion demands relatively lengthy periods of activity (Hickey et al. 2013), and the synchrony promoted by electrical coupling may ensure that all neurons spike sufficiently for optimal release of reproductive hormone.

#### ACKNOWLEDGMENTS

We thank N. M. Magoski for critical evaluation of previous drafts of the manuscript.

#### GRANTS

Z. Dargaei held a Queen's Graduate Award. This work was supported by a Natural Sciences and Engineering Research Council of Canada Discovery Grant (to N. S. Magoski).

#### DISCLOSURES

No conflicts of interest, financial or otherwise, are declared by the author(s).

#### AUTHOR CONTRIBUTIONS

Author contributions: Z.D., P.L.W.C., H.M.H., and N.S.M. performed experiments; Z.D., P.L.W.C., H.M.H., and N.S.M. analyzed data; Z.D., P.L.W.C., and N.S.M. interpreted results of experiments; Z.D., P.L.W.C., and N.S.M. prepared figures; Z.D., P.L.W.C., and N.S.M. edited and revised manuscript; Z.D., P.L.W.C., H.M.H., and N.S.M. approved final version of manuscript; N.S.M. conception and design of research; N.S.M. drafted manuscript.

#### REFERENCES

- Andrew RD, MacVicar BA, Dudek FE, Hatton GI. Dye transfer through gap junctions between neuroendocrine cells of rat hypothalamus. *Science* 211: 1187–1189, 1981.
- Arch S. Polypeptide secretion from the isolated parietovisceral ganglion of *Aplysia californica*. *J Gen Physiol* 59: 47–59, 1972.
- Beblo DA, Veenstra RD. Monovalent cation permeation through the connexin40 gap junction channel. Cs, Rb, K, Na, Li, TEA, TMA, TBA, and effects of anions Br, Cl, F, acetate, aspartate, glutamate, and NO<sub>3</sub>. *J Gen Physiol* 109: 509–522, 1997.
- Benjamin PR, Pilkington JB. The electrotonic location of low-resistance intercellular junctions between a pair of giant neurones in the snail *Lymnaea*. *J Physiol* 370: 111–126, 1986.
- Bennett MV. Physiology of electrotonic junctions. *Ann NY Acad Sci* 137: 509–539, 1966.
- Bennett MV. Electrical transmission: a functional analysis and comparison with chemical transmission. In: *Handbook of Physiology. The Nervous System. Cellular Biology of Neurons*. edited by Kandel ER. Bethesda, MD: Am Physiol Soc, 1977, vol. I, p. 357–416.
- Bennett MV. Seeing is relieving: electrical synapses between visualized neurons. *Nat Neurosci* 3: 7–9, 2000.
- Bennett MV, Zukin RS. Electrical coupling and neuronal synchronization in the mammalian brain. *Neuron* 41: 495–511, 2004.
- Bezaniilla F, Armstrong CM. Inactivation of the sodium channel. I. Sodium current experiments. *J Gen Physiol* 70: 549–566, 1977.
- Belin V, Moos F. Paired recordings from supraoptic and paraventricular oxytocin cells in suckled rats: recruitment and synchronization. *J Physiol* 377: 369–390, 1986.
- Berry MS, Pentreath VW. Criteria for distinguishing between monosynaptic and polysynaptic transmission. *Brain Res* 105: 1–20, 1976.
- Blankenship J, Haskins J. Electrotonic coupling among neuro-endocrine cells in *Aplysia*. *J Neurophysiol* 42: 347–355, 1979.
- Bodmer R, Verselis V, Levitan IB, Spray DC. Electrotonic synapses between *Aplysia* neurons in situ and in culture: aspects of regulation and measurements of permeability. *J Neurosci* 8: 1656–1670, 1988.
- Brown RO, Mayeri E. Positive feedback by autoexcitatory neuropeptides in neuroendocrine bag cells of *Aplysia*. *J Neurosci* 9: 1443–1451, 1989.

- Brown RO, Pulst SM, Mayeri E.** Neuroendocrine bag cells of *Aplysia* are activated by bag cell peptide-containing neurons in the pleural ganglion. *J Neurophysiol* 61: 1142–1152, 1989.
- Bukauskas FF, Verselis VK.** Gap junction channel gating. *Biochim Biophys Acta* 1662: 42–60, 2004.
- Cao G, Nitabach MN.** Circadian control of membrane excitability in *Drosophila melanogaster* lateral ventral clock neurons. *J Neurosci* 28: 6493–6501, 2008.
- Carew TJ, Kandel ER.** Inking in *Aplysia californica*. I. Neural circuit of an all-or-none behavioral response. *J Neurophysiol* 40: 692–707, 1977.
- Carrow GM, Levitan IB.** Selective formation and modulation of electrical synapses between cultured *Aplysia* neurons. *J Neurosci* 9: 3657–3664, 1989.
- Carter CJ, Magoski NS.** Electrical coupling in *Aplysia*: identification of innexin genes. *Can Assoc Neurosci Abstr* 8: 1-B-24, 2014.
- Coggeshall RE.** A light and electron microscope study of the abdominal ganglion of *Aplysia californica*. *J Neurophysiol* 30: 1263–1287, 1967.
- Colwell CS.** Rhythmic coupling among cells in the suprachiasmatic nucleus. *J Neurobiol* 43: 379–388, 2000.
- Conn PJ, Kaczmarek LK.** The bag cell neurons of *Aplysia*. *Mol Neurobiol* 3: 237–273, 1989.
- Davidson JS, Baumgarten IM.** Glycylrrhethinic acid derivatives: a novel class of inhibitors of gap-junctional intercellular communication. Structure-activity relationships. *J Pharmacol Exp Ther* 246: 1104–1107, 1988.
- De Vlieger TA, Kits KS, Ter Maat A, Lodder JC.** Morphology and electrophysiology of the ovulation hormone producing neuro-endocrine cells of the freshwater snail *Lymnaea stagnalis* (L.). *J Exp Biol* 84: 259–271, 1980.
- Desarménien MG, Jourdan C, Toutain B, Vessières E, Hormuzdi SG, Guérineau NC.** Gap junction signaling is a stress-regulated component of adrenal neuroendocrine stimulus-secretion coupling in vivo. *Nat Commun* 4: 2938, 2013.
- Deschênes M, Bennett MV.** A qualification to the use of TEA as a tracer for monosynaptic pathways. *Brain Res* 77: 169–172, 1974.
- Dudek FE, Blankenship JE.** Neuroendocrine cells of *Aplysia brasiliana*. I. Bag cell action potentials and afterdischarge. *J Neurophysiol* 40: 1301–1311, 1977.
- Dudek FE, Cobbs JS, Pinsker HM.** Bag cell electrical activity underlying spontaneous egg laying in freely behaving *Aplysia brasiliana*. *J Neurophysiol* 42: 804–817, 1979.
- Dykes IM, Freeman FM, Bacon JP, Davies JA.** Molecular basis of gap junctional communication in the CNS of the leech *Hirudo medicinalis*. *J Neurosci* 24: 886–894, 2004.
- Ermentrout B, Wang J, Flores J, Gelperin A.** Model for transition from waves to synchrony in the olfactory lobe of *Limax*. *J Comput Neurosci* 17: 365–383, 2004.
- Esikandari S, Zampighi GA, Leung DW, Wright EM, Loo DD.** Inhibition of gap junction hemichannels by chloride channel blockers. *J Membr Biol* 185: 93–102, 2002.
- Ewadinger NM, Syed NI, Lukowiak K, Bulloch AG.** Differential tracer coupling between pairs of identified neurones of the mollusc, *Lymnaea stagnalis*. *J Exp Biol* 192: 291–297, 1994.
- Fan RJ, Marin-Burgin A, French KA, Friesen WO.** A dye mixture (Neurobiotin and Alexa 488) reveals extensive dye-coupling among neurons in leeches; physiology confirms the connections. *J Comp Physiol A* 191: 1157–1171, 2005.
- Frazier WT, Kandel ER, Kupfermann I, Waziri R, Coggeshall RE.** Morphological and functional properties of identified neurons in the abdominal ganglion of *Aplysia californica*. *J Neurophysiol* 30: 1288–1351, 1967.
- Furshpan EJ, Potter DD.** Transmission at the giant motor synapses of the crayfish. *J Physiol* 145: 289–325, 1959.
- Gardam KE, Geiger JE, Hickey CM, Hung AY, Magoski NS.** Flufenamic acid affects multiple currents and causes intracellular  $Ca^{2+}$  release in *Aplysia* bag cell neurons. *J Neurophysiol* 100: 38–49, 2008.
- Geiger JE, Magoski NS.**  $Ca^{2+}$ -induced  $Ca^{2+}$ -release in *Aplysia* bag cell neurons requires interaction between mitochondrial and endoplasmic reticulum stores. *J Neurophysiol* 100: 24–37, 2008.
- Getting PA.** Modification of neuron properties by electrotonic synapses. I. Input resistance, time constant and integration. *J Neurophysiol* 37: 816–857, 1974.
- Getting PA, Willows AO.** Modification of neuron properties by electrotonic synapses. II. Burst formation by electrotonic synapses. *J Neurophysiol* 37: 858–868, 1974.
- Gibson JR, Beierlein M, Connors BW.** Two networks of electrically coupled inhibitory neurons in neocortex. *Nature* 402: 75–79, 1999.
- Gögelein H, Dahlem D, Englert HC, Lang HJ.** Flufenamic acid, mefenamic acid and niflumic acid inhibit single nonselective cation channels in the rat exocrine pancreas. *FEBS Lett* 268: 79–82, 1990.
- Hamill OP, Marty A, Neher E, Sakmann B, Sigworth FJ.** Improved patch-clamp techniques for high-resolution current recording from cells and cell-free membrane patches. *Pflügers Arch* 391: 85–100, 1981.
- Harks EG, de Roos AD, Peters PH, de Haan LH, Brouwer A, Ypey DL, van Zoelen EJ, Theuvsen AP.** Fenamates: a novel class of reversible gap junction blockers. *J Pharmacol Exp Ther* 298: 1033–1041, 2001.
- Haskins JT, Blankenship JE.** Interactions between bilateral clusters of neuroendocrine cells in *Aplysia*. *J Neurophysiol* 42: 356–367, 1979.
- Hatcher NG, Sweedler JV.** *Aplysia* bag cells function as a distributed neurosecretory network. *J Neurophysiol* 99: 333–343, 2008.
- Hickey CM, Geiger KE, Groten CJ, Magoski NS.** Mitochondrial  $Ca^{2+}$  activates a cation current in *Aplysia* bag cell neurons. *J Neurophysiol* 103: 1543–1556, 2010.
- Hickey CM, Groten CJ, Sham L, Carter CJ, Magoski NS.** Voltage-gated  $Ca^{2+}$  influx and mitochondrial  $Ca^{2+}$  initiate secretion from *Aplysia* neuroendocrine cells. *Neuroscience* 250: 755–772, 2013.
- Hille B.** *Ionic Channels of Excitable Membranes*. Sunderland, MA: Sinauer Associates, 2001.
- Heitzmann H, Richards FM.** Use of the avidin-biotin complex for specific staining of biological membranes in electron microscopy. *Proc Natl Acad Sci USA* 71: 3537–3541, 1974.
- Horikawa K, Armstrong WE.** A versatile means of intracellular labeling: injection of biocytin and its detection with avidin conjugates. *J Neurosci Methods* 25: 1–11, 1988.
- Hung AY, Magoski NS.** Activity-dependent initiation of a prolonged depolarization in *Aplysia* bag cell neurons: Role for a cation channel. *J Neurophysiol* 97: 2465–2479, 2007.
- Kachoei BA, Knox RJ, Uthuzza D, Levy S, Kaczmarek LK, Magoski NS.** A store-operated  $Ca^{2+}$  influx pathway in the bag cell neurons of *Aplysia*. *J Neurophysiol* 96: 2688–2698, 2006.
- Johnston MF, Simon SA, Ramon R.** Interaction of anaesthetics with electrical synapses. *Nature* 286: 498–500, 1980.
- Juszczak GR, Swiergiel AH.** Properties of gap junction blockers and their behavioural, cognitive and electrophysiological effects: animal and human studies. *Prog Neuropsychopharmacol Biol Psychiatry* 33: 181–198, 2009.
- Kaczmarek LK, Finbow M, Revel JR, Strumwasser F.** The morphology and coupling of *Aplysia* bag cells within the abdominal ganglion and in cell culture. *J Neurobiol* 10: 535–550, 1979.
- Katz B, Miledi R.** The timing of calcium action during neuromuscular transmission. *J Physiol* 189: 535–544, 1967.
- Kupfermann I, Kandel ER, Coggeshall R.** Synchronized activity in neurosecretory cell cluster in *Aplysia*. *Physiologist* 9: 223, 1966.
- Kupfermann I, Kandel ER.** Electrophysiological properties and functional interconnections of two symmetrical neurosecretory clusters (bag cells) in abdominal ganglion of *Aplysia*. *J Neurophysiol* 33: 865–876, 1970.
- Landisman CE, Long MA, Beierlein M, Deans MR, Paul DL, Connors BW.** Electrical synapses in the thalamic reticular nucleus. *J Neurosci* 22: 1002–1009, 2002.
- Levitan H, Tauc L, Segundo JP.** Electrical transmission among neurons in the buccal ganglion of a mollusc, *Navanax inermis*. *J Gen Physiol* 55: 484–496, 1970.
- Lin SS, Levitan IB.** Concanavalin A alters synaptic specificity between cultured *Aplysia* neurons. *Science* 237: 648–650, 1987.
- Liu Q, Chen B, Gaier E, Joshi J, Wang ZW.** Low conductance gap junctions mediate specific electrical coupling in body-wall muscle cells of *Caenorhabditis elegans*. *J Biol Chem* 277: 7881–7889, 2002.
- Linás R, Steinberg IZ, Walton K.** Relationship between presynaptic calcium current and postsynaptic potential in squid giant synapse. *Biophys J* 33: 323–351, 1981.
- Loechner KJ, Kaczmarek LK.** Autoactive peptides act at three distinct receptors to depolarize the bag cell neurons of *Aplysia*. *J Neurophysiol* 71: 195–203, 1994.
- Long MA, Jutras MJ, Connors BW, Burwell RD.** Electrical synapses coordinate activity in the suprachiasmatic nucleus. *Nature Neurosci* 8: 61–66, 2005.
- Lupinsky DA, Magoski NS.**  $Ca^{2+}$ -dependent regulation of a non-selective cation channel from *Aplysia* bag cell neurones. *J Physiol* 575: 491–506, 2006.
- Magoski NS, Knox RJ, Kaczmarek LK.** Activation of a  $Ca^{2+}$ -permeable cation channel produces a prolonged attenuation of intracellular  $Ca^{2+}$  release in *Aplysia* bag cell neurons. *J Physiol* 522: 271–283, 2000.

- Magoski NS, Kaczmarek LK.** Association/dissociation of a channel-kinase complex underlies state-dependent modulation. *J Neurosci* 25: 8037–8047, 2005.
- Martin AO, Mathieu MN, Chevillard C, Guerineau NC.** Gap junctions mediate electrical signalling and ensuing cytosolic  $Ca^{2+}$  increases between chromaffin cells in adrenal slices: a role in catecholamine release. *J Neurosci* 21: 5397–5405, 2001.
- Mayeri E, Brownell P, Branton WD, Simon SB.** Multiple, prolonged actions of neuroendocrine bag cells on neurons in *Aplysia*. I. Effects on bursting pacemaker neurons. *J Neurophysiol* 42: 1165–1184, 1979a.
- Mayeri E, Brownell P, Branton WD.** Multiple, prolonged actions of neuroendocrine bag cells on neurons in *Aplysia*. II. Effects on beating pacemaker and silent neurons. *J Neurophysiol* 42: 1185–1197, 1979b.
- McCracken CB, Roberts DC.** Neuronal gap junctions: expression, function, and implications for behavior. *Int Rev Neurobiol* 73: 125–151, 2006.
- Michel S, Wayne NL.** Neurohormone secretion persists after post-afterdischarge membrane depolarization and cytosolic calcium elevation in peptidergic neurons in intact nervous tissue. *J Neurosci* 22: 9063–9069, 2002.
- Moroz LL, Edwards JR, Puthanveetil SV, Kohn AB, Ha T, Heyland A, Knudsen B, Sahni A, Yu F, Liu L, Jezzini S, Lovell P, Iannuccilli W, Chen M, Nguyen T, Sheng H, Shaw R, Kalachikov S, Panchin YV, Farmerie W, Russo JJ, Ju J, Kandel ER.** Neuronal transcriptome of *Aplysia*: neuronal compartments and circuitry. *Cell* 127: 1453–1467, 2006.
- Murphy AD, Hadley RD, Kater SB.** Axotomy-induced parallel increases in electrical and dye coupling between identified neurons of *Helisoma*. *J Neurosci* 3: 1422–1429, 1983.
- Neyton J, Trautmann A.** Single-channel currents of an intercellular junction. *Nature* 317: 331–335, 1985.
- Norekian TP.** GABAergic excitatory synapses and electrical coupling sustain prolonged discharges in the prey capture neural network of *Clione limacina*. *J Neurosci* 19: 1863–1875, 1999.
- Obaid AL, Socolar SJ, Rose B.** Cell-to-cell channels with two independent regulated gates in series: analysis of junctional channel modulation by membrane potential, calcium and pH. *J Membr Biol* 73: 69–89, 1983.
- Pan F, Mills SL, Massey SC.** Screening of gap junction antagonists on dye coupling in the rabbit retina. *Vis Neurosci* 24: 609–618, 2007.
- Payton BW, Bennett MV, Pappas GD.** Permeability and structure of junctional membranes at an electrotonic synapse. *Science* 166: 1641–1643, 1969.
- Peinado A, Yuste R, Katz LC.** Extensive dye coupling between rat neocortical neurons during the period of circuit formation. *Neuron* 10: 103–114, 1993.
- Phelan P, Goulding LA, Tam JL, Allen MJ, Dawber RJ, Davies JA, Bacon JP.** Molecular mechanism of rectification at identified electrical synapses in the *Drosophila* giant fiber system. *Curr Biol* 18: 1955–1960, 2008.
- Poronnik P, Ward MC, Cook DI.** Intracellular  $Ca^{2+}$  release by flufenamic acid and other blockers of the non-selective cation channel. *FEBS Lett* 296: 245–248, 1992.
- Rothman BS, Weir G, Dudek FE.** Egg-laying hormone: direct action on the ovotestis of *Aplysia*. *Gen Comp Endocrinol* 52: 134–141, 1983.
- Sieling F, Bédécarrats A, Simmers J, Prinz AA, Nargeot R.** Differential roles of nonsynaptic and synaptic plasticity in operant reward learning-induced compulsive behavior. *Curr Biol* 24: 941–950, 2014.
- Solomon IC, Chon KH, Rodriguez MN.** Blockade of brain stem gap junctions increases phrenic burst frequency and reduces phrenic burst synchronization in adult rat. *J Neurophysiol* 89: 135–149, 2003.
- Spencer A.** The parameters and properties of a group of electrically coupled neurones in the central nervous system of a hydrozoan jellyfish. *J Exp Biol* 93: 33–50, 1981.
- Spray DC, Harris AL, Bennett MV.** Voltage dependence of junctional conductance in early amphibian embryos. *Science* 204: 432–434, 1979.
- Srinivas M, Hopperstad MG, Spray DC.** Quinine blocks specific gap junction channel subtypes. *Proc Natl Acad Sci USA* 98: 10942–10947, 2001.
- Srinivas M, Spray DC.** Closure of gap junction channels by arylaminobenzoates. *Mol Pharmacol* 63: 1389–1397, 2003.
- Stewart WW.** Functional connections between cells as revealed by dye-coupling with a highly fluorescent naphthalimide tracer. *Cell* 14: 741–59, 1978.
- Strong JA, Kaczmarek LK.** Multiple components of delayed potassium current in peptidergic neurons of *Aplysia*: modulation by an activator of adenylate cyclase. *J Neurosci* 6: 814–822, 1986.
- Stuart DK, Chiu AY, Strumwasser F.** Neurosecretion of egg-laying hormone and other peptides from electrically active bag cell neurons of *Aplysia*. *J Neurophysiol* 43: 488–498, 1980.
- Stuart DK, Strumwasser F.** Neuronal sites of action of a neurosecretory peptide, egg-laying hormone, in *Aplysia californica*. *J Neurophysiol* 43: 499–519, 1980.
- Summerlee A.** Extracellular recordings from oxytocin neurones during the expulsive phase of birth in unanesthetized rats. *J Physiol* 321: 1–9, 1981.
- Takahira M, Sakurai M, Sakurada N, Sugiyama K, Fenamates and diltiazem modulate lipid-sensitive mechano-gated 2P domain  $K^{+}$  channels. *Pflügers Arch* 451: 474–478, 2005.**
- Tam AK, Geiger JE, Hung AY, Groten CJ, Magoski NS.** Persistent  $Ca^{2+}$  current contributes to a prolonged depolarization in *Aplysia* bag cell neurons. *J Neurophysiol* 102: 3753–3765, 2009.
- Tam AK, Gardam KE, Lamb S, Kachoei BA, Magoski NS.** Role for protein kinase C in controlling *Aplysia* bag cell neuron excitability. *Neuroscience* 179: 41–55, 2011.
- Traub RD, Kopell N, Bibbig A, Buhl EH, LeBeau FE, Whittington MA.** Gap junctions between interneuron dendrites can enhance synchrony of gamma oscillations in distributed networks. *J Neurosci* 21: 9478–9486, 2001.
- Vazquez-Martinez R, Shorte SL, Boockfor FR, Frawley LS.** Synchronized exocytotic bursts from gonadotropin-releasing hormone-expressing cells: dual control by intrinsic cellular pulsatility and gap junctional communication. *Endocrinology* 142: 2095–2101, 2001.
- Verselis V, White RL, Spray DC, Bennett MV.** Gap junctional conductance and permeability are linearly related. *Science* 234: 461–464, 1986.
- Waziri R.** Electrical transmission mediated by an identified cholinergic neuron of *Aplysia*. *Life Sci* 8: 469–476, 1969.
- White MM, Aylwin M.** Niflumic and flufenamic acids are potent reversible blockers of  $Ca^{2+}$ -activated  $Cl^{-}$  channels in *Xenopus* oocytes. *Mol Pharmacol* 37: 720–724, 1990.
- White TW, Wang H, Muia R, Litteral J, Brink PR.** Cloning and functional expression of invertebrate connexins from *Halocynthia pyriformis*. *FEBS Lett* 577: 42–48, 2004.
- White SH, Magoski NS.** Acetylcholine-evoked afterdischarge in *Aplysia* bag cell neurons. *J Neurophysiol* 107: 2672–2685, 2012.
- White SH, Carter CJ, Magoski NS.** A potentially novel nicotinic receptor in *Aplysia* neuroendocrine cells. *J Neurophysiol* 112: 446–462, 2014.
- Wildering WC, van der Roest M, de Vlieger TA, Janse C.** Age-related changes in junctional and non-junctional conductances in two electrically coupled peptidergic neurons of the mollusc *Lymnaea stagnalis*. *Brain Res* 547: 89–98, 1991.
- Wildering WC, Janse C.** Serotonergic modulation of junctional conductance in an identified pair of neurons in the mollusc *Lymnaea stagnalis*. *Brain Res* 595: 343–352, 1992.
- Wu JS, Wang N, Siniscalchi MJ, Perkins MH, Zheng YT, Yu W, Chen SA, Jia RN, Gu JW, Qian YQ, Ye Y, Vilim FS, Cropper EC, Weiss KR, Jing J.** Complementary interactions between command-like interneurons that function to activate and specify motor programs. *J Neurosci* 34: 6510–6521, 2014.